transfected cells were transferred to complete DMEM and cultured for the indicated period. Cells were passaged every 3–5 days; the presence of HCV in these cells and corresponding supernatants were determined at the indicated time points.

RNA Analysis. Total cellular RNA was isolated by the guanidine thiocyanate method by using standard protocols (32). RT-QPCR analysis (for primer sequences, see Fig. 7, which is published as supporting information on the PNAS web site) was performed as described (19, 33), and HCV and GAPDH transcript levels were determined relative to a standard curve comprised of serial dilutions of plasmid containing the HCV JFH-1 cDNA or human GAPDH gene.

Indirect Immunofluorescence. Intracellular staining was performed as described (33). Polyclonal anti-NS5A rabbit antibody MS5 [a gift from Michael Houghton (Chiron)] was used at a dilution of 1:1,000 followed by incubation with a 1:1,000 dilution of Alexa555-conjugated goat anti-rabbit IgG (Molecular Probes) for 1 h at room temperature. Cell nuclei were stained by Hoechst dye.

Titration of Infectious HCV. Cell supernatants were serially diluted 10-fold in complete DMEM and used to infect 10^4 naïve Huh-7.5.1 cells per well in 96-well plates (Corning). The inoculum was incubated with cells for 1 h at 37°C and then supplemented with fresh complete DMEM. The level of HCV infection was determined 3 days postinfection by immunofluorescence staining for HCV NS5A. The viral titer is expressed as focus-forming units per milliliter of supernatant (ffu/ml), determined by the average number of NS5A-positive foci detected at the highest dilutions.

Amplification of HCV Viral Stocks. To generate viral stocks, infectious supernatants were diluted in complete DMEM and used to inoculate naïve 10–15% confluent Huh-7.5.1 cells at an moi of 0.01 in a T75 flask (Corning). Infected cells were trypsinized and replated before confluence at day 4–5 postinfection (p.i.). Supernatant from infected cells was then harvested 8–9 days p.i. and aliquoted for storage at −80°C. The titer of viral stock was determined as described above.

Concentration and Purification of HCV. Sucrose density-gradient ultracentrifugation analysis was performed as described (34). Pooled supernatant from two mock or two HCV-infected T162 cm^2 Costar flasks (Corning) were centrifuged at 4,000 rpm for 5 min to remove cellular debris and then pelleted through a 20% sucrose cushion at 28,000 rpm for 4 h by using a SW28 rotor in an L8–80M ultracentrifuge (Beckman). The pellet was resuspended in 1 ml of TNE buffer (50 mM Tris·HCl, pH 8/100 mM NaCl/1 mM EDTA) containing protease inhibitors (Roche Applied Science, Indianapolis), loaded onto a 20–60% sucrose gradient (12.5-ml total volume), and centrifuged at 120,000 × *g* for 16 h at 4°C in a SW41Ti rotor (Beckman). Fractions of 1.3 ml were collected from the top of the gradient. The fractions were analyzed by RT-QPCR to detect HCV RNA. To determine the infectivity titer of each fraction, fractions were titrated on Huh7.5.1 cells as described above.

Blocking Infection with CD81- and E2-Specific Antibodies. Recombinant human monoclonal (IgG1) anti-E2 antibody was derived from a cDNA expression library (prepared from mononuclear cells of a HCV patient) that was screened against recombinant HCV genotype 1a E2 protein (GenBank accession no. M62321) by phage display. The antibody was serially diluted and preincubated with 15,000 ffu of JFH-1 virus in a volume of 250 μl for 1 h at 37°C. The virus antibody mixture was then used to infect 45,000 Huh-7.5.1 cells in a 24-well plate (Corning) for 3 h at 37°C. Mouse monoclonal anti-human CD81 antibody 5A6 (35) at 1 mg/ml (a gift from Shoshana Levy, Stanford University, Stanford, CA) was serially diluted (1:2,000, 1:200, and 1:20) and preincubated in a volume of 50 μl with 10^4 Huh-7.5.1 cells seeded in a 96-well plate for 1 h at 37°C. Cells were subsequently inoculated with infectious JFH-1 supernatant at an moi of 0.3 for 3 h at 37°C. The efficiency of the infection in the presence of antibodies was monitored 3 days p.i. by RT-QPCR and immunofluorescence.

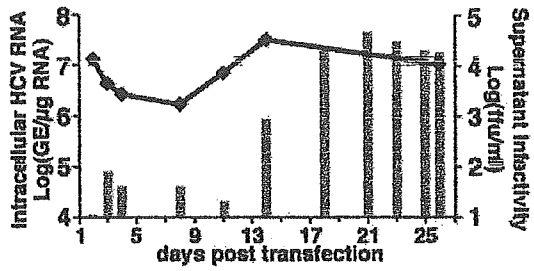

Fig. 1. Production of infectious HCV after transfection of genomic JFH-1 RNA. Ten micrograms of *in vitro* transcribed JFH-1 RNA was electroporated into 4×10^6 Huh-7.5.1 cells. Transfected cells and supernatant were harvested at the indicated time points posttransfection. Intracellular HCV RNA was analyzed by RT-QPCR and displayed as genome equivalents (GE)/μg total RNA (line). Supernatant infectivity titers were determined in naïve Huh-7.5.1 cells and are expressed as ffu/ml (bars).

Results

Production of Infectious HCV Particles in HCV RNA-Transfected Hepatoma Cells. Blight *et al.* (36) have established an Huh-7-derived cell line, termed Huh-7.5, that is highly permissive for replication of HCV replicons, including the I/5A-GFP-6 replicon (30) that expresses an NS5A-GFP fusion protein. For the current study, we cured I/5A-GFP-6 replicon cells with IFN-γ (see *Materials and Methods*) establishing an HCV-negative Huh-7.5-derived cell line, which we refer to as Huh-7.5.1. In a first set of experiments, 10 μg of *in vitro* transcribed genomic JFH-1 RNA was delivered into Huh-7.5.1 cells by electroporation. Transfected cells were then passaged when necessary (usually every 3–4 days) to maintain subconfluent cultures throughout the experiment. At the indicated times, total RNA was isolated from the transfected Huh-7.5.1 cells, and the level of HCV RNA was determined by HCV-specific RT-QPCR. Two days posttransfection, 1.3×10^7 copies of HCV RNA per μg of cellular RNA were detected (Fig. 1), probably reflecting a combination of input RNA and RNA produced by intracellular HCV replication. HCV RNA levels subsequently decreased, reaching a minimum level of 1.6×10^6 copies per μg of cellular RNA at day 8 posttransfection (Fig. 1). Importantly, however, intracellular HCV RNA levels began to increase thereafter, reaching maximal levels of $>10^7$ copies per μg of total RNA by day 14 posttransfection, and these levels were maintained until the experiment was terminated on day 26 (Fig. 1). These results suggested that HCV was actively replicating in transfected Huh-7.5.1 cells. This notion is supported by a rapid disappearance of a replication-incompetent JFH-1 RNA genome after transfection (Fig. 7).

Interestingly, immunofluorescence staining for NS5A indicated that the percentage of NS5A-positive cells in the transfected cell cultures increased from 2% on day 5 (Fig. 2*A*) to almost 100% on day 24 (Fig. 2*B*). These results were consistent with the amplification of HCV RNA and further suggested either that HCV-transfected cells had acquired a selective growth advantage or that HCV was spreading to untransfected cells within the culture.

To determine whether the JFH-1-transfected Huh-7.5.1 cells were releasing infectious virus, we inoculated naïve Huh-7.5.1

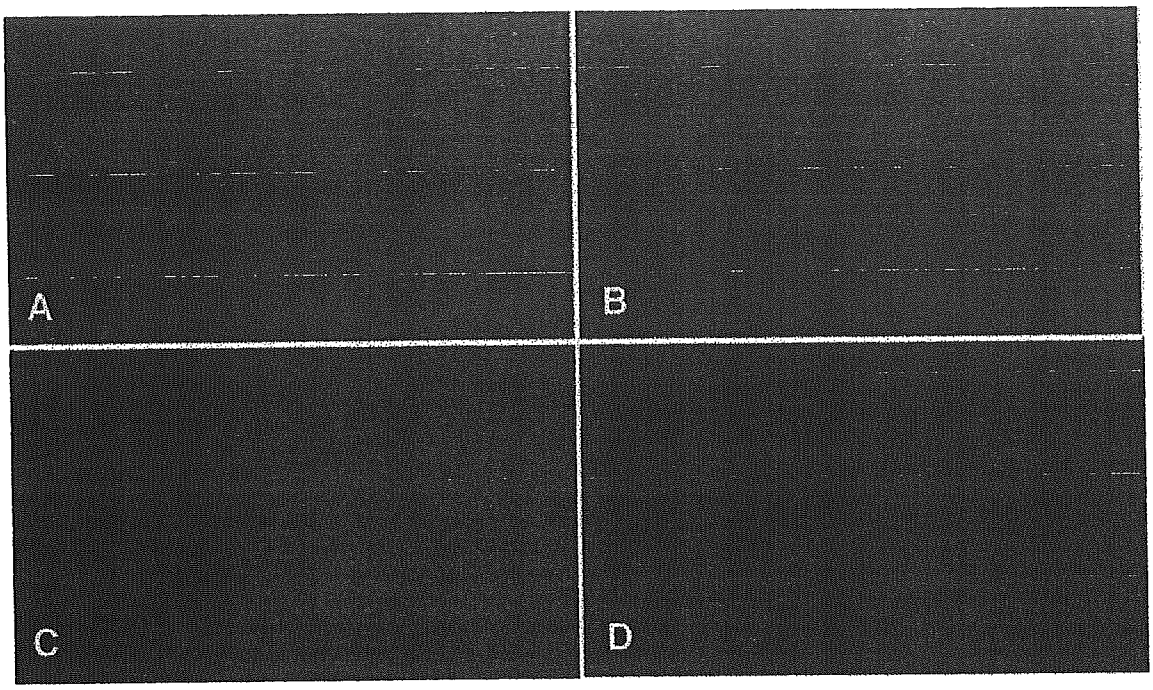

Fig. 2. Detection of infected cells by NS5A immunofluorescence. (*Upper*) Immunofluorescent detection of NS5A in transfected cells: (*A*) day 5 and (*B*) day 24 posttransfection. (*Lower*) Infectivity titration of transfected cell supernatant on naïve Huh-7.5.1 cells; (*C*) undiluted supernatant; (*D*) 10-fold diluted supernatant. NS5A staining in red; nuclei stained with Hoechst (blue) (×50).

cells with supernatants collected at different time points during the transfection experiment. Not only did immunofluorescence staining 3 days postinoculation reveal NS5A positive cells in the culture (Fig. 2*C*) but also, when the supernatants were serially diluted, the infection resulted in discrete foci of NS5A-positive cells (Fig. 2*D*), which allowed us to determine the ffu/ml in the supernatants collected at different times posttransfection. This type of supernatant titration was performed for the transfection experiment described in Fig. 1 and is indicated by vertical bars (Fig. 1). Infectious virus was detected in the culture medium 3 days after transfection (80 ffu/ml) and then increased, reaching a maximum of 4.6×10^4 ffu/ml by day 21 posttransfection, concomitant with the amplification of intracellular JFH-1 RNA.

Taken together, these results strongly suggest that Huh-7.5.1 cells transfected with genomic JFH-1 RNA were able not only to support HCV replication but also to produce infectious HCV particles. Notably, similar results were obtained when JFH-1 RNA was delivered to Huh-7.5.1 cells by an alternative transfection method (i.e., liposomes; Fig. 8, which is published as supporting information on the PNAS web site).

Propagation of HCV Virus Generated by Transfection. Next, we determined whether cells infected with JFH-1-transfected cell supernatant produced progeny virus that could be serially passaged to naïve Huh-7.5.1 cells. To do so, we infected naive Huh-7.5.1 cells at low multiplicity (moi = 0.01) with infectious supernatants collected from two independent transfection experiments and monitored infectious virus production by titrating the infected cell supernatants at the indicated time points. On day 1 after inoculation, no infectious particles were detectable in the supernatant of cells infected with either transfection cell inoculate (Fig. 3*A*). However, infectious particles exponentially accumulated in the supernatant thereafter, reaching a maximal titer of at least 10^4 ffu/ml on day 7 after both infections (Fig. 3*A*). Thus, within 7 days p.i., HCV produced in two independent transfection experiments was amplified in naïve Huh-7.5.1 cells >100-fold with very similar kinetics. Of note, we also performed additional experiments in which we monitored the intracellular levels of HCV RNA and proteins. This analysis confirmed that the appearance of infectious virus in the cell culture supernatant directly correlated with the amplification and subsequent translation of the input HCV RNA (Fig. 9, which is published as supporting information on the PNAS web site).

To determine whether the progeny virus produced by infection could be further passaged, we infected naive Huh-7.5.1 cells with the virus collected from one of the experiments shown in Fig. 3*A* (lipofection). As shown in Fig. 3*B*, this secondary infection progressed with kinetics similar to the primary infection (Fig. 3*A*), again reaching maximal levels on day 7. This was reflected by increasing numbers of NS5A-positive cells over the time course of the infection, with almost all of the cells being positive for NS5A at day 7 (Fig. 3*C*). These results indicate that the JFH-1 virus generated by transfection can be passaged in Huh-7.5.1 cells without a detectable loss in infectivity, and that it infects a high proportion of the cells in a relatively short period.

HCV Infection Is Inhibited by Anti-E2 Antibodies. Previous studies using HCV surface glycoprotein (E1/E2) pseudotyped viruses (37, 38) have suggested that E1 and/or E2 mediate the interaction with cellular receptors that are required for viral adsorption. To verify whether such an interaction is required for HCV infection *in vitro*, we performed neutralization experiments using anti-E2 antibodies in which the JFH-1 virus was preincubated with serial dilutions of a recombinant human monoclonal antibody specific for HCV E2 or an isotype-negative control antibody for 3 h at 37°C before infection.

Huh-7.5.1 cells infected with JFH-1 virus (moi = 0.3) in the presence of 100 μg/ml of anti-E2 antibody were found to have 5-fold lower intracellular HCV RNA levels compared with cells infected in the presence of the same amount of an isotype control antibody (Fig. 4*A*), and this was reflected by a reduction in NS5A-positive cells as determined by immunofluorescence

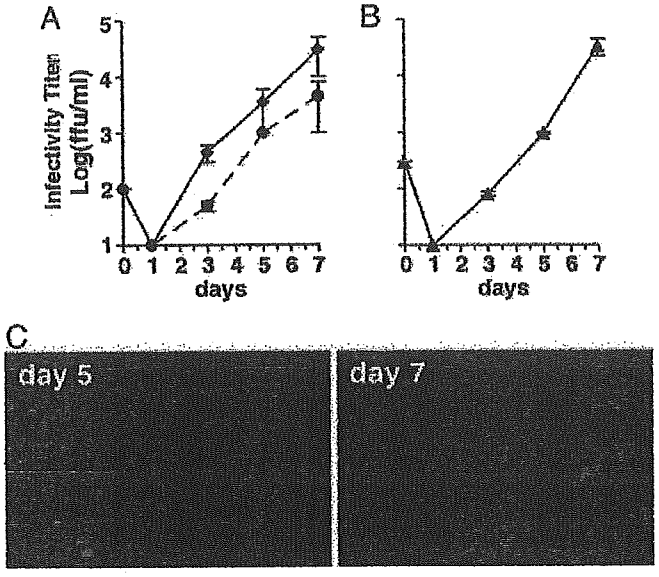

Fig. 3. HCV infection kinetics and passage in tissue culture cells. Naïve Huh 7.5.1 cells were inoculated with culture supernatants at an moi of 0.01. Supernatants from the inoculated cells were collected at the indicated times p.i. and evaluated for infectivity (ffu/ml). Data represent the average of two or more experiments with error bars. (*A*) Huh-7.5.1 cells inoculated with supernatant harvested at day 19 after transfection of Huh-7.5.1 cells with JFH-1 genomic RNA by electroporation (dashed line) or day 24 after lipofection (solid line). (*B*) Huh-7.5.1 cells inoculated with supernatant collected at day 5 from the infection shown as a solid line in *A*; (*C*) increasing NS5A immunostaining in Huh-7.5.1 cells between days 5 and 7 p.i. in the experiment shown in *B*.

(data not shown). Titration of the anti-E2 antibody indicated that 10 μg/ml of antibody was required for a 50% reduction in intracellular HCV RNA 3 days p.i. (Fig. 4*A*). These results are therefore consistent with the conclusion that *in vitro* HCV infection in this system is at least in part mediated by the viral envelope E2 protein.

HCV Infection Is Inhibited by Anti-CD81 Antibodies. Previous studies using pseudotyped viruses that express HCV E1/E2 have also suggested that the interaction between HCV E2 and CD81 is crucial for viral entry (39). To determine whether CD81 is required in this HCV infection system, anti-CD81 antibody-pretreated naïve Huh-7.5.1 were infected with JFH-1 virus at an moi of 0.3 and analyzed 3 days p.i. Intracellular HCV RNA levels

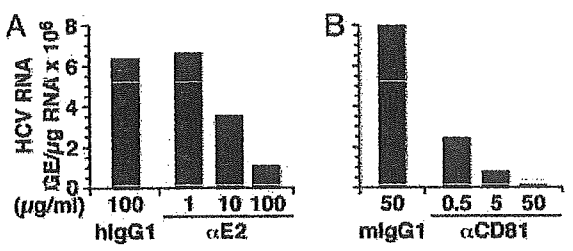

Fig. 4. Inhibition of HCV infection by anti-E2 and anti-CD81 antibodies. (*A*) JFH-1 virus was preincubated with the indicated concentrations of anti-E2 antibody or irrelevant human IgG1 antibody for 1 h at 37°C before inoculating Huh-7.5.1 cells. Total cellular RNA was analyzed by RT-QPCR at day 3 p.i. (*B*) Huh-7.5.1 cells were preincubated with the indicated concentrations of anti-human CD81 or control mouse IgG1 antibody for 1 h at 37°C before inoculation with JFH-1 virus at an moi of 0.3. Total cellular RNA was analyzed by RT-QPCR at day 3 p.i.

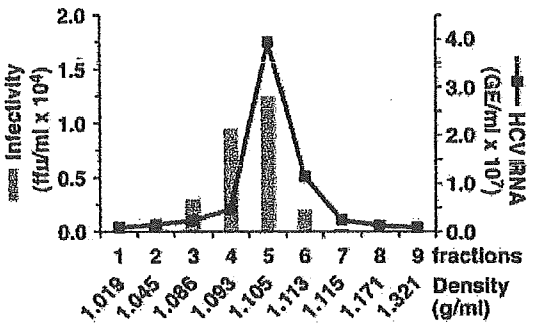

Fig. 5. Sucrose gradient sedimentation of infectious HCV. Supernatant from infected Huh-7.5.1 cells was fractionated as described in *Materials and Methods*. Fractions (1–9) were collected from the top of the gradient and analyzed by RT-QPCR for HCV RNA (line). The infectivity of each fraction was determined (bars) by titration. Fraction densities are expressed as g/ml.

were reduced in a dose-dependent manner with a 50-fold reduction at 50 μg/ml anti-CD81 antibody compared with the control antibody-treated cells (Fig. 4*B*).

Biophysical Properties of Infectious HCV JFH-1 Particles. To examine the density of the secreted infectious HCV virions, supernatants collected from uninfected and HCV-infected Huh7.5.1 cells were subjected to sucrose gradient centrifugation. Gradient fractions were collected after centrifugation and analyzed for the presence of HCV RNA and infectivity (Fig. 5). Maximal infectivity titers (1.25×10^4 ffu/ml) were present in fraction 5 and coincided with the peak of HCV RNA. The ≈1.105 g/ml apparent density of the peak infectivity fraction is consistent with that previously reported for HCV virions isolated from patient sera (40, 41), indicating that the density of the recombinant JFH-1 virus is similar to that of human isolates.

***In Vitro* Tropism of JFH-1 HCV.** To determine whether infection with the JFH-1 virus was restricted to Huh-7.5.1 cells, we attempted to infect a panel of hepatic (Huh-7 and HepG2) and nonhepatic cell lines (HeLa, HEK293, HL-60, U-937, and EBV-transformed B cells). Besides the Huh-7.5.1 cells, only the Huh-7 cells were permissive for HCV infection, as determined by immunofluorescent staining for the viral NS5A protein at day 3 p.i. (data not shown).

To determine whether there are quantitative differences in infection efficiency between the Huh-7.5.1 and Huh-7 cells, we infected both cell lines in parallel. As shown in Fig. 6, infectious particle release into the supernatant of infected Huh-7 cells

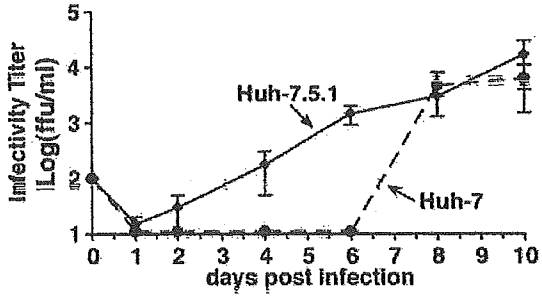

Fig. 6. Kinetics of JFH-1 HCV infection in Huh-7.5.1 and Huh-7 cells. A virus stock generated in Huh-7.5.1 was diluted to infect Huh-7.5.1 and Huh-7 cells at an moi of 0.01. Culture supernatant was collected at the indicated times and titrated. Infectious titers in Huh-7.5.1 (solid lines) and Huh-7 cells (dashed lines) are expressed as ffu/ml. Average values of two independent infection experiments are shown.

MICROBIOLOGY

appears to be delayed when compared with the particle production by Huh-7.5.1 cells. Nevertheless, Huh-7 cells produced similar amounts of infectious particles by days 8 and 10. Similar delayed kinetics in the amplification of intracellular HCV RNA was also observed in the Huh-7 cells (Fig. 10, which is published as supporting information on the PNAS web site). Taken together, these results demonstrate that Huh-7 cells can produce similar amounts of progeny virus as Huh-7.5.1 cells but with delayed kinetics.

Discussion

The absence of a robust cell culture model of HCV infection has limited the analysis of the HCV life cycle and the development of effective antivirals and vaccines. Despite intensive efforts by many groups and the finding that *in vitro* transcribed HCV RNA is infectious when transfected into the liver of chimpanzees (42, 43), production of infectious HCV *in vitro* has remained problematic. Although a cell line capable of producing HCV-like virions was recently reported, the infectivity of those particles was not demonstrated (34). Furthermore, until recently, the replication efficiency of HCV replicons has depended on adaptive mutations (reviewed in ref. 44) that are attenuating in chimpanzees (45).

Interestingly, Kato *et al.* (22) produced an HCV genotype 2a replicon (JFH-1) that replicates efficiently in Huh-7 cells without adaptive mutations. Importantly, Wakita *et al.* (26, ‖) have also reported that JFH-1 RNA generated from the genomic JFH-1 viral clone can produce virus when transfected into Huh-7 cells. The limitation of this discovery has been the low efficiency of infection achieved and the resulting inability to perform controlled infection experiments.

Here, we report the establishment of a simple yet robust cell culture HCV infection system based on the reverse genetics system designed by Wakita *et al.* (26, ‖), which allows the rescue of infectious virus from the JFH-1 consensus cDNA clone. Our results demonstrate that transfection of JFH-1 RNA into the Huh-7-derived cells allows for the recovery of a viable JFH virus that can then be serially passaged and used for infection-based experimentation. Impressively, infection with serial dilutions of the virus resulted in the formation of infected cell foci that allowed us to quantitatively titrate the HCV being produced. Although the molecular basis of this viral spread pattern requires additional investigation, one can speculate that after infection at low multiplicity, HCV may spread by multiple mechanisms such as by attaching preferentially to adjacent cells after secretion and/or by spreading via cell-to-cell transmission.

The ability to monitor the complete HCV infection process *in vitro* has already provided some insight into the HCV life cycle. Specifically, the disappearance of input virus from the supernatant within 24 h p.i. suggests that particles were able to enter the cells within this time frame. As infectious viral titers rose from these undetected levels to 10^4-10^5 ffu/ml, the number of NS5A-positive cells also increased, suggesting that the virus was spreading to new cells (Fig. 3C). Importantly, when passaged to naïve Huh-7.5.1 cells, the virus produced by both transfected and infected cells exhibited the same infection kinetics with an HCV doubling time of ≈22 h. This doubling time is longer than the 6–8 h previously reported in infected patients (46) and chimpanzees (47); however, technical and biological factors may be responsible for this discrepancy. For example, earlier estimates were based on the number of HCV genome equivalents detected in the serum of infected individuals, not the infectivity titer as in the current study. The different doubling times may also reflect genotypic differences between the infecting viruses in the various studies and/or biological differences between Huh-7.5.1 cells and primary hepatocytes in the context of the liver.

The tropism of the JFH-1 virus thus far appears to be limited to Huh-7-derived cell lines. Even HepG2, HeLa, and HEK293 cells, which have been shown to support replication of the subgenomic JFH-1 replicon (22, 24, 25), failed to become infected. This suggests that the block to HCV infection in these cells may exist before RNA replication and translation. Importantly, that an antibody directed against the viral surface glycoprotein E2 reduced the infectivity of the JFH-1 virus suggests the process of viral adsorption and entry can be studied in this system. Consistent with this claim, HCV infection of Huh-7-derived cells was inhibited by an antibody against CD81 (Fig. 4), an extensively characterized putative HCV receptor (48).

Our initial efforts focused on the use of Huh7.5.1 cells, a cell line derived from Huh7.5 cells that has been shown to be highly permissive for HCV genotype 1 replicon replication (36). Importantly, however, non-HCV-adapted Huh-7 cells were also found to be susceptible to infection with the JFH-1 virus (Fig. 6). Virus amplification in Huh-7 cells did tend to display slower kinetics, but the Huh-7 cells eventually produced viral titers comparable to those attained in Huh-7.5.1 cells. The specific characteristics of the Huh-7.5.1 cells might be crucial in the future, because we expect mutants with reduced viability to be produced during reverse genetics studies investigating HCV biology.

Although the different kinetics of virus production in these two Huh-7-based cell lines is still under continued investigation, at this point, the differences observed are compatible with the idea that HCV infection may induce an innate antiviral response in the Huh-7 cells that is compromised in the Huh-7.5.1 cells. Specifically, it has been demonstrated that Huh-7.5 cells contain an inactivating mutation in RIG-I (49), a key component of the cellular double-stranded RNA-sensing machinery (50). Hence, our results suggest that HCV infection may induce a double-stranded RNA antiviral defense pathway in the Huh-7 cells, which transiently delays viral replication and/or spread. That HCV eventually overcomes the limitations present in Huh-7 cells and reaches titers similar to those produced by Huh-7.5.1 cells further suggests that expression of one or more viral encoded functions (e.g., NS3 or NS5A) may block or negate the intracellular antiviral defense(s). HCV infection, however, remained sensitive to the effects of exogenously added IFN, because both IFN-α and -γ prevented JFH-1 virus infection of Huh-7.5.1 cells (Fig. 11, which is published as supporting information on the PNAS web site). Interestingly, these *in vitro* observations appear to parallel those seen clinically (5, 46, 51), in which IFN therapy is able to reduce viral titers in some patients regardless of the mechanisms the virus has evolved that allow it to persist in the presence of the IFN it induces. Ongoing comparison of HCV infection in these different Huh-7-based cell lines should provide a unique opportunity to dissect and understand these critical virus–host interactions.

Conclusion

We have established a robust cell culture model of HCV infection in which infectious HCV can be produced and serially passaged to naïve cells. The availability of this system creates the opportunity to address aspects of the virus life cycle, including entry, trafficking, viral assembly, and egress, that have not been previously approachable. Likewise, many aspects of the host–virus relationship can now be explored, particularly the proviral factors that are required for viral production and the antiviral factors that control HCV infection. In addition to the deeper understanding of basic HCV infection biology that should be forthcoming from this system, it creates new investigative opportunities that could greatly accelerate the discovery of antiviral drugs and contribute to the development of an HCV vaccine.

We thank Dr. Charles Rice (Rockefeller University, New York) and Dr. Darius Moradpour (University of Lausanne, Lausanne, Switzer-

land) for providing the I/5A-GFP-6 replicon cell line, Dr. Rice for information about the susceptibility of Huh-7.5 cells to HCV infection before publication, and Dr. Shoshana Levy (Stanford University, Stanford, CA) for providing anti-CD81 antibodies. This study was supported by Grants CA108304 (to F.V.C.) and AI060391 (to S.L.U.) from the National Institutes of Health and by the Sam and Rose Stein Charitable Trust. S.K. was supported by the American Cancer Society–Gloria Rosen Postdoctoral Research Fellowship. T.W. was supported by the Program for Promotion of Fundamental Studies in Health Sciences of the Pharmaceuticals and Medical Devices Agency (PMDA) and by the Research on Health Sciences focusing on Drug Innovation from the Japan Health Sciences Foundation. This is manuscript number 17387-MEM from The Scripps Research Institute.

1. Hoofnagle, J. H. (2002) *Hepatology* **36,** S21–S29.
2. Kanto, T., Hayashi, N., Takehara, T., Tatsumi, T., Kuzushita, N., Ito, A., Sasaki, Y., Kasahara, A. & Hori, M. (1999) *J. Immunol.* **162,** 5584–5591.
3. Auffermann-Gretzinger, S., Keeffe, E. B. & Levy, S. (2001) *Blood* **97,** 3171–3176.
4. Hiasa, Y., Horiike, N., Akbar, S. M., Saito, I., Miyamura, T., Matsuura, Y. & Onji, M. (1998) *Biochem. Biophys. Res. Commun.* **249,** 90–95.
5. Alter, H. J. & Seeff, L. B. (2000) *Semin. Liver Dis.* **20,** 17–35.
6. Thimme, R., Oldach, D., Chang, K. M., Steiger, C., Ray, S. C. & Chisari, F. V. (2001) *J. Exp. Med.* **194,** 1395–1406.
7. Takaki, A., Wiese, M., Maertens, G., Depla, E., Seifert, U., Liebetrau, A., Miller, J. L., Manns, M. P. & Rehermann, B. (2000) *Nat. Med.* **6,** 578–582.
8. Lechner, F., Wong, D. K., Dunbar, P. R., Chapman, R., Chung, R. T., Dohrenwend, P., Robbins, G., Phillips, R., Klenerman, P. & Walker, B. D. (2000) *J. Exp. Med.* **191,** 1499–1512.
9. Logvinoff, C., Major, M. E., Oldach, D., Heyward, S., Talal, A., Balfe, P., Feinstone, S. M., Alter, H., Rice, C. M. & McKeating, J. A. (2004) *Proc. Natl. Acad. Sci. USA* **101,** 10149–10154.
10. Shoukry, N. H., Sidney, J., Sette, A. & Walker, C. M. (2004) *J. Immunol.* **172,** 483–492.
11. Thimme, R., Bukh, J., Spangenberg, H. C., Wieland, S., Pemberton, J., Steiger, C., Govindarajan, S., Purcell, R. H. & Chisari, F. V. (2002) *Proc. Natl. Acad. Sci. USA* **99,** 15661–15668.
12. Bukh, J. (2004) *Hepatology* **39,** 1469–1475.
13. Ikeda, M., Yi, M., Li, K. & Lemon, S. M. (2002) *J. Virol.* **76,** 2997–3006.
14. Lohmann, V., Korner, F., Koch, J., Herian, U., Theilmann, L. & Bartenschlager, R. (1999) *Science* **285,** 110–113.
15. Gale, M., Jr. (2003) *Hepatology* **37,** 975–978.
16. Katze, M. G., He, Y. & Gale, M., Jr. (2002) *Nat. Rev. Immunol.* **2,** 675–687.
17. Dubuisson, J. & Rice, C. M. (1996) *J. Virol.* **70,** 778–786.
18. Ye, J., Wang, C., Sumpter, R., Jr., Brown, M. S., Goldstein, J. L. & Gale, M., Jr. (2003) *Proc. Natl. Acad. Sci. USA* **100,** 15865–15870.
19. Kapadia, S. B. & Chisari, F. V. (2005) *Proc. Natl. Acad. Sci. USA* **102,** 2561–2566.
20. Lohmann, V., Korner, F., Dobierzewska, A. & Bartenschlager, R. (2001) *J. Virol.* **75,** 1437–1449.
21. Blight, K. J., Kolykhalov, A. A. & Rice, C. M. (2000) *Science* **290,** 1972–1975.
22. Kato, T., Date, T., Miyamoto, M., Furusaka, A., Tokushige, K., Mizokami, M. & Wakita, T. (2003) *Gastroenterology* **125,** 1808–1817.
23. Kato, T., Furusaka, A., Miyamoto, M., Date, T., Yasui, K., Hiramoto, J., Nagayama, K., Tanaka, T. & Wakita, T. (2001) *J. Med. Virol.* **64,** 334–339.
24. Date, T., Kato, T., Miyamoto, M., Zhao, Z., Yasui, K., Mizokami, M. & Wakita, T. (2004) *J. Biol. Chem.* **279,** 22371–22376.
25. Kato, T., Date, T., Miyamoto, M., Zhao, Z., Mizokami, M. & Wakita, T. (2005) *J. Virol.* **79,** 592–596.
26. Wakita, T., Pietschmann, T., Kato, T., Date, T., Miyamoto, M., Zhao, Z., Murthy, K., Habermann, A., Krausslich, H. G., Mizokami, M., Bartenschlager, R. & Liang, T. J. (2005) *Nat. Med.*, in press.
27. Graham, F. L., Smiley, J., Russell, W. C. & Nairn, R. (1977) *J. Gen. Virol.* **36,** 59–74.
28. Gey, G. O., Coffman, W. D. & Kubicek, M. T. (1952) *Cancer Res.* **12,** 264–265.
29. Knowles, B. B., Howe, C. C. & Aden, D. P. (1980) *Science* **209,** 497–499.
30. Moradpour, D., Evans, M. J., Gosert, R., Yuan, Z., Blum, H. E., Goff, S. P., Lindenbach, B. D. & Rice, C. M. (2004) *J. Virol.* **78,** 7400–7409.
31. Krieger, N., Lohmann, V. & Bartenschlager, R. (2001) *J. Virol.* **75,** 4614–4624.
32. Chomczynski, P. & Sacchi, N. (1987) *Anal. Biochem.* **162,** 156–159.
33. Kapadia, S. B., Brideau-Andersen, A. & Chisari, F. V. (2003) *Proc. Natl. Acad. Sci. USA* **100,** 2014–2018.
34. Heller, T., Saito, S., Auerbach, J., Williams, T., Moreen, T. R., Jazwinski, A., Cruz, B., Jeurkar, N., Sapp, R., Luo, G. & Liang, T. J. (2005) *Proc. Natl. Acad. Sci. USA* **102,** 2579–2583.
35. Levy, S., Todd, S. C. & Maecker, H. T. (1998) *Annu. Rev. Immunol.* **16,** 89–109.
36. Blight, K. J., McKeating, J. A. & Rice, C. M. (2002) *J. Virol.* **76,** 13001–13014.
37. Bartosch, B., Dubuisson, J. & Cosset, F. L. (2003) *J. Exp. Med.* **197,** 633–642.
38. Hsu, M., Zhang, J., Flint, M., Logvinoff, C., Cheng-Mayer, C., Rice, C. M. & McKeating, J. A. (2003) *Proc. Natl. Acad. Sci. USA* **100,** 7271–7276.
39. Zhang, J., Randall, G., Higginbottom, A., Monk, P., Rice, C. M. & McKeating, J. A. (2004) *J. Virol.* **78,** 1448–1455.
40. Hijikata, M., Shimizu, Y. K., Kato, H., Iwamoto, A., Shih, J. W., Alter, H. J., Purcell, R. H. & Yoshikura, H. (1993) *J. Virol.* **67,** 1953–1958.
41. Trestard, A., Bacq, Y., Buzelay, L., Dubois, F., Barin, F., Goudeau, A. & Roingeard, P. (1998) *Arch. Virol.* **143,** 2241–2245.
42. Yanagi, M., Purcell, R. H., Emerson, S. U. & Bukh, J. (1997) *Proc. Natl. Acad. Sci. USA* **94,** 8738–8743.
43. Kolykhalov, A. A., Agapov, E. V., Blight, K. J., Mihalik, K., Feinstone, S. M. & Rice, C. M. (1997) *Science* **277,** 570–574.
44. Bartenschlager, R., Kaul, A. & Sparacio, S. (2003) *Antiviral Res.* **60,** 91–102.
45. Bukh, J., Pietschmann, T., Lohmann, V., Krieger, N., Faulk, K., Engle, R. E., Govindarajan, S., Shapiro, M., St Claire, M. & Bartenschlager, R. (2002) *Proc. Natl. Acad. Sci. USA* **99,** 14416–14421.
46. Neumann, A. U., Lam, N. P., Dahari, H., Gretch, D. R., Wiley, T. E., Layden, T. J. & Perelson, A. S. (1998) *Science* **282,** 103–107.
47. Tanaka, J., Katayama, K., Kumagai, J., Komiya, Y., Yugi, H., Kishimoto, S., Mizui, M., Tomoguri, T., Miyakawa, Y. & Yoshizawa, H. (2005) *Intervirology* **48,** 120–123.
48. Cormier, E. G., Tsamis, F., Kajumo, F., Durso, R. J., Gardner, J. P. & Dragic, T. (2004) *Proc. Natl. Acad. Sci. USA* **101,** 7270–7274.
49. Sumpter, R., Jr., Loo, Y. M., Foy, E., Li, K., Yoneyama, M., Fujita, T., Lemon, S. M. & Gale, M., Jr. (2005) *J. Virol.* **79,** 2689–2699.
50. Yoneyama, M., Kikuchi, M., Natsukawa, T., Shinobu, N., Imaizumi, T., Miyagishi, M., Taira, K., Akira, S. & Fujita, T. (2004) *Nat. Immunol.* **5,** 730–737.
51. Mbow, M. L. & Sarisky, R. T. (2004) *Trends Biotechnol.* **22,** 395–399.

TECHNICAL REPORTS

nature medicine

Production of infectious hepatitis C virus in tissue culture from a cloned viral genome

Takaji Wakita[1,7], Thomas Pietschmann[2,7], Takanobu Kato[1,3,4], Tomoko Date[1], Michiko Miyamoto[1], Zijiang Zhao[1], Krishna Murthy[5], Anja Habermann[6], Hans-Georg Kräusslich[6], Masashi Mizokami[3], Ralf Bartenschlager[2,7] & T Jake Liang[4]

Hepatitis C virus (HCV) infection causes chronic liver diseases and is a global public health problem. Detailed analyses of HCV have been hampered by the lack of viral culture systems. Subgenomic replicons of the JFH1 genotype 2a strain cloned from an individual with fulminant hepatitis replicate efficiently in cell culture. Here we show that the JFH1 genome replicates efficiently and supports secretion of viral particles after transfection into a human hepatoma cell line (Huh7). Particles have a density of about 1.15–1.17 g/ml and a spherical morphology with an average diameter of about 55 nm. Secreted virus is infectious for Huh7 cells and infectivity can be neutralized by CD81-specific antibodies and by immunoglobulins from chronically infected individuals. The cell culture–generated HCV is infectious for chimpanzee. This system provides a powerful tool for studying the viral life cycle and developing antiviral strategies.

HCV is a major cause of chronic liver diseases[1,2]. Development of selectable drugs and efficient vaccines has been hampered by poor virus growth in cell culture[3]. Although subgenomic replicons replicate efficiently in cultured cells[4], for unknown reasons infectious viral particles are not produced[5,6]. Subgenomic replicons of the HCV genotype 2a JFH1 strain cloned from an individual with fulminant hepatitis[7] replicate efficiently in Huh7 cells and do not require cell culture–adaptive mutations[8–10]. In this study, we show that transfection of *in vitro*–transcribed full-length JFH1 RNA into Huh7 cells results in secretion of viral particles that are infectious for cultured cells and a chimpanzee.

RESULTS

Virus production from cells transfected with full-length JFH1 RNA

We transfected *in vitro*–transcribed RNAs corresponding to the full-length JFH1 genome (**Fig. 1a**) and a replication-incompetent mutant (JFH1/GND) into Huh7 cells. Total RNAs from cells harvested at different time points were analyzed by northern hybridization (**Fig. 1b**). Up to 12 h after transfection, we detected only degraded input RNA. But genome-length RNA was found in JFH1-transfected cells after 24 h, and remained detectable up to 72 h. The same was true for expression of viral proteins (**Fig. 1c** and **Supplementary Fig. 1** online). Immunofluorescence analysis of JFH1-transfected cells showed that 70–80% of the cells were positive for core and nonstructural (NS) 3 proteins at 72 h after transfection (**Fig. 1d**), indicating that this genome replicates to high levels in transfected Huh7 cells.

As a surrogate for virus production, we quantified secretion of core protein into the culture medium of cells transfected with JFH1 mutants JFH/GND and JFH1/ΔE1-E2 or full-length genomes of different origin (J6CF[11] or JCH1 (ref. 7)). Core protein was secreted efficiently from JFH1 RNA but much less efficiently from JFH1/ΔE1-E2 RNA–transfected cells (**Fig. 1e**), despite comparable core protein levels. No core protein was secreted from the other RNA-transfected cells, consistent with their lack of replication (data not shown). These results suggest that core secretion depends on HCV RNA replication and that envelope glycoproteins are required, although the RNA segment deleted in JFH1/ΔE1-E2 may contain signal(s) required for core secretion.

To determine whether JFH1 RNA–transfected cells can sustain continuous HCV replication, we serially passaged cells. Cells transfected with JFH1/ΔE1-E2 RNA or a subgenomic replicon (SGR-JFH1)[8] lacking the core to NS2 region served as controls. We determined HCV RNA titer using real-time detection reverse transcription (RTD)-PCR[12]. In JFH1-transfected cells, viral RNA and core protein titers in the medium increased rapidly at 5 d after transfection, and remained high for the next 7 d, followed by a slow decrease (**Fig. 2a**). In contrast, RNA levels in supernatant of control cells gradually decreased with increasing passage. At day 30, background levels were reached, which were 4.5% for JFH1/ΔE1-E2– and 0.7% for SGR-JFH1 RNA–transfected cells as compared to JFH1 (**Fig. 2a**). During the first two passages, transfected cells had similar levels of intracellular HCV RNA, but they declined much more rapidly in the controls (**Fig. 2a**). We also determined levels of core protein and obtained similar results (**Supplementary Fig. 2**

[1]Department of Microbiology, Tokyo Metropolitan Institute for Neuroscience, Tokyo 183-8526, Japan. [2]Department of Molecular Virology, University Heidelberg, Im Neuenheimer Feld 345, 69120 Heidelberg, Germany. [3]Department of Clinical Molecular Informative Medicine, Nagoya City University Graduate School of Medical Sciences, Nagoya 467-8601, Japan. [4]Liver Disease Branch, NIDDK, National Institute of Health, Bethesda, Maryland 20892, USA. [5]Southwest Foundation for Biomedical Research, San Antonio, Texas, 78227, USA. [6]Department of Virology, University of Heidelberg, Im Neuenheimer Feld 324, 69120 Heidelberg, Germany. [7]These authors contributed equally to this work. Correspondence should be addressed to T.W. (wakita@tmin.ac.jp).

Published online 12 June 2005; doi:10.1038/nm1268

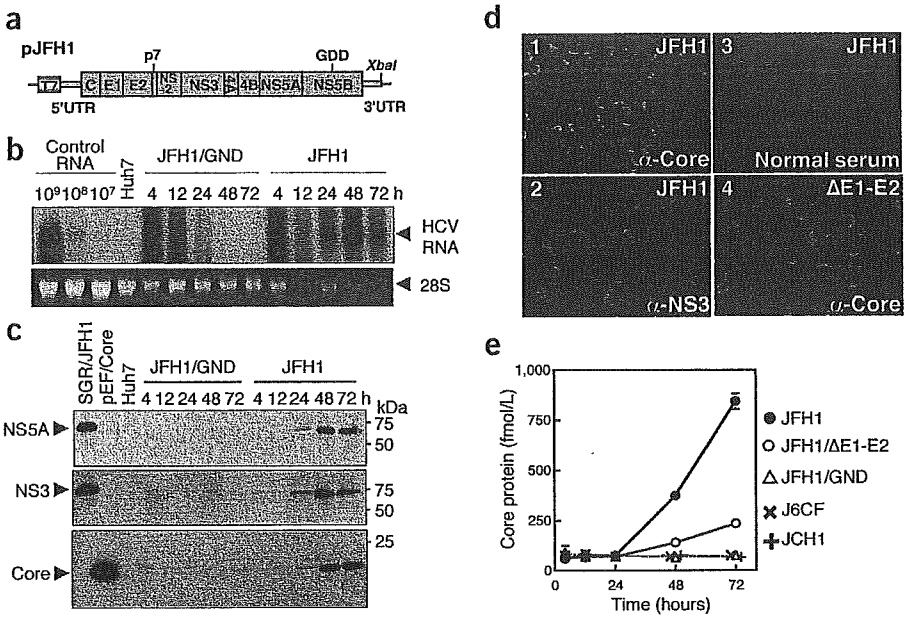

Figure 1 Transient replication of JFH1 RNA in transfected Huh7 cells. (**a**) Organization of the full-length HCV construct pJFH1. Open reading frames (thick boxes) are flanked by the 5′- and 3′-UTRs (thin boxes). T7, T7 RNA polymerase promoter; GDD, active-site motif of NS5B polymerase; *XbaI*, restriction site. (**b**) Northern blot analysis of total RNA prepared from cells transfected with full-length JFH1 and JFH1/GND RNA. Control RNA, given numbers of synthetic HCV RNA; Huh7, RNA isolated from naive cells. Arrowheads indicate full-length HCV RNA and 28S ribosomal RNA (28S). Upper panel, northern blot; lower panel, ethidium bromide staining. (**c**) Western blot analysis of transfected cells for HCV proteins NS5A, NS3 and core. Lysates of SGR/JFH1-RNA[8] or pEF/Core[29] DNA–transfected Huh7 cells and naive Huh7 cells served as positive and negative controls, respectively. (**d**) Immunofluorescence assay of cells fixed 72 h after transfection with JFH1 (1–3) or JFH1/ΔE1-E2 RNA (4). Magnification, ×200. (**e**) HCV core protein secretion into culture medium after HCV transfection of Huh7 cells.

online). Immunofluorescence assay showed that 3 d after transfection, JFH1 RNA and JFH1/ΔE1-E2 RNA transfection gave similar numbers of HCV-positive cells (**Fig. 1d**). After 13 d, 50–60% of JFH1 RNA–transfected cells were still positive for core protein, but only a few with the mutant (**Fig. 2b**). These results indicate a limited spread of infection. Alternatively, JFH1 RNA–replicating cells may have a longer half-life than cells containing JFH1/ΔE1-E2 or SGR-JFH1 RNAs.

Biophysical properties of HCV particles

To characterize secreted viral particles, we analyzed supernatant of JFH1-transfected cells using a sucrose density gradient. Core protein and nuclease-resistant HCV RNA sedimented to the same density of 1.17 g/ml (**Supplementary Fig. 3** online). To show co-sedimentation of all structural proteins, we generated a JFH1-E2HA construct containing a hemagglutinin tag replacing part of the E2 hypervariable region (HVR). HCV lacking the HVR is infectious in chimpanzee[13], and JFH1-E2HA virus remained infectious for Huh7 cells. Similar to the wild type, viral particles of this mutant had a density of ~1.15 g/ml (**Fig. 3a**). Moreover, we detected core, E1 and E2 proteins in the same peak fraction of the sucrose density gradient (**Fig. 3b**), indicating the production of complete viral particles.

Detection of HCV particles by electron microscopy

Cell culture–derived JFH1 particles were visualized by immunoelectron microscopy, using an E2-specific antibody (CBH5)[14]. We detected gold-labeled spherical structures with an electron-dense inner core using a concentrated virus preparation (**Fig. 3c–e**), whereas we found only unstructured aggregates with the mock-transfected control (**Fig. 3f**). The inner ring has a slightly angular morphology and a diameter of 30–35 nm, consistent with nucleocapsids[15]. The overall diameter of the structures (50–65 nm) is compatible with the predicted size of HCV[15–18].

Infectivity of HCV particles

We inoculated naive Huh7 cells with supernatant harvested from JFH1 RNA– or JFH1/ΔE1-E2 RNA–transfected cells, and 48 h later we double-stained cells for core and NS5A (**Fig. 4a**). Only cells inoculated with JFH1 medium were positive for these proteins (10–20 cells/cover slip, **Fig. 4a**), with the number increasing to about 390 core protein–positive cells/cover slip using 1/30 concentrated medium (~0.5% of inoculated cells; **Fig. 4a**). To exclude the possibility that residual *in vitro* transcripts were captured by inoculated cells, we prepared supernatant from cells treated with the same amount of JFH1 RNA but without the electroporation. Upon inoculation of naive Huh7 cells, we observed no core protein–positive cells (**Fig. 4a**), as was the case with supernatant from JFH1/ΔE1-E2 RNA–transfected cells. Furthermore, ultraviolet irradiation of the inoculum substantially reduced the number of positive cells. Finally, we found no productive infection with HepG2, IMY-N9 and HeLa cells (**Fig. 4a**), consistent with their lower permissiveness for HCV RNA replication[9,10].

To compare infectivity of culture supernatant of JFH1 RNA– and JFH1/ΔE1-E2 RNA–transfected cells, we inoculated Huh7 cells with concentrates containing equivalent RNA copy numbers (1.17×10^8 copies/ml) and determined amounts of cell-associated RNA at 0, 12, 24 and 48 h after inoculation. We detected similar amounts of RNA in cells after an adsorption period of 3 h and found similar decreases up to 12 h (**Fig. 4b**). But 12 h later, RNA titers increased only in JFH1-inoculated cells, suggesting that productive infection depends on HCV envelope glycoproteins (**Fig. 4b**). This conclusion was supported by results obtained with single E-gene deletions (**Supplementary Fig. 4** online). JFH1-E2HA particles were also infectious for Huh7 cells, but the RNA titer in infected cells was approximately 10 times lower compared to JFH1 virus infection (data not shown). Finally, HCV can be passaged by infection but virus titers decrease upon serial passages (data not shown).

Neutralization of HCV infection by CD81-specific antibody

CD81 was shown to be involved in HCV entry using HCV pseudoparticles[19,20]. To determine whether authentic particles follow the same entry route and to confirm specificity of uptake, we incubated Huh7 cells with JFH1 or JFH1/ΔE1-E2 inocula in the presence of CD81-specific or nonspecific antibodies. We scored infection 48 h later, using NS3-specific immunofluorescence (**Supplementary Fig. 5** online) or RTD-PCR (**Fig. 4c**). CD81-specific antibodies reduced both the number of infected cells and the amount of HCV RNA associated with the cells by about 90% as compared to control antibody, confirming specificity of the infection and the important role of CD81 in HCV entry.

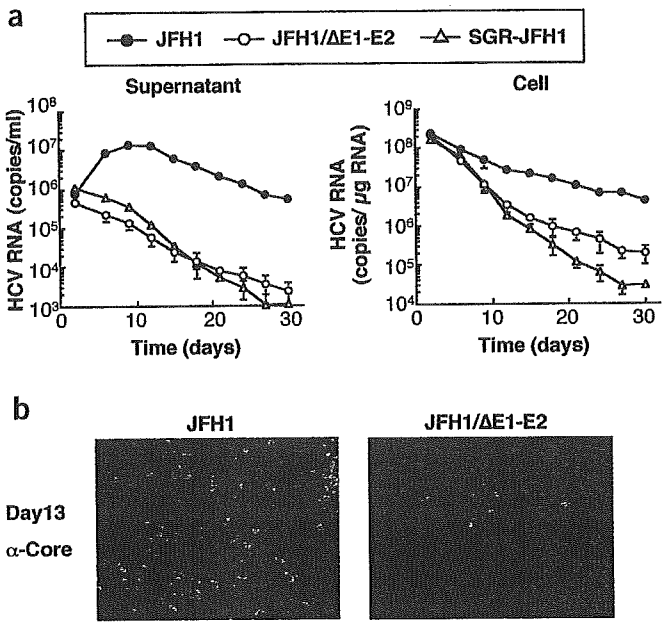

Figure 2 Time course of HCV RNA replication and core protein expression in transfected cells. (a) Levels of HCV RNA in transfected cells (right) and corresponding culture supernatants (left). Huh7 cells were transfected with given HCV RNAs and passaged up to 30 d. Viral RNA was determined 2, 5, 8, 12, 15, 18, 21, 24, 27 and 30 d after transfection. (b) Immunofluorescence assay of HCV core protein in passaged cells transfected with JFH1 and JFH1/ΔE1-E2 RNA. Transfected cells were harvested 1 d after the fourth passage (day 13 after transfection). Magnification, ×100.

Neutralization of infection by patient sera

To facilitate quantification of infection, we generated a bicistronic JFH1 luciferase reporter construct (**Fig. 4d** and **Supplementary Fig. 6** online). Infectious titers attainable by JFH1 and Luc-JFH1 genomes are similar, indicating that added sequences do not markedly affect production of infectious particles (data not shown). Taking advantage of this system, we performed neutralization experiments using sera of individuals infected with HCV genotype 2 or 1. Culture supernatants containing Luc-JFH1 virus particles were mixed with serum dilutions and infection was determined by luciferase assay (we considered a reduction to at least 50% significant). At a dilution of 1:20, all HCV sera showed neutralizing activity comparable to 0.08 μg/ml CD81-specific antibody (**Fig. 4d**). Neutralization was dose dependent and highest with sera 3 and 4. None of the serum samples inhibited entry of HIV-based pseudoparticles bearing murine leukemia virus–derived envelope proteins into Huh7 (data not shown). Finally, antibodies purified from patient 3 but not from control serum B inhibited infection with similar efficiency as the original serum, whereas immunoglobulin depletion prevented neutralization (**Fig. 4d**). These data show that antibodies in sera from infected individuals are capable of neutralizing JFH1 viruses.

Infectivity of cell culture–derived HCV particles *in vivo*

To show the infectivity of cell culture–grown JFH1 virus *in vivo*, we intravenously inoculated medium from JFH1 RNA transfected cells into a chimpanzee. The inoculum contained 7.65×10^6 RNA copies/ml and had a core protein concentration of 4,630 fmol/L. To ensure that the HCV RNA remaining in the medium after transfection did not cause infection, we collected medium from a mock-transfected culture, in which HCV RNA was added to the cells without transfection. This sample contained 3.47×10^4 RNA copies/ml and had undetectable levels of core protein. Chimpanzee X0205 was inoculated with 1 ml of undiluted control medium and showed no signs of infection for 6 weeks (**Fig. 5**). Thereafter, we inoculated the chimpanzee with 1 ml of a 10^4 dilution of supernatant from JFH1 RNA–transfected cells. After 6 weeks of monitoring with no signs of infection, we re-inoculated the chimpanzee with 1 ml of a 10^3 dilution. HCV RNA became detectable in the serum at week 2, persisted until week 5, and thereafter became undetectable. Viremia was low with highest HCV RNA titer of 2.04×10^3 copies/ml at week 4. Infection was cleared without HCV-specific seroconversion, elevation of alanine aminotransferase or histological evidence of liver injury

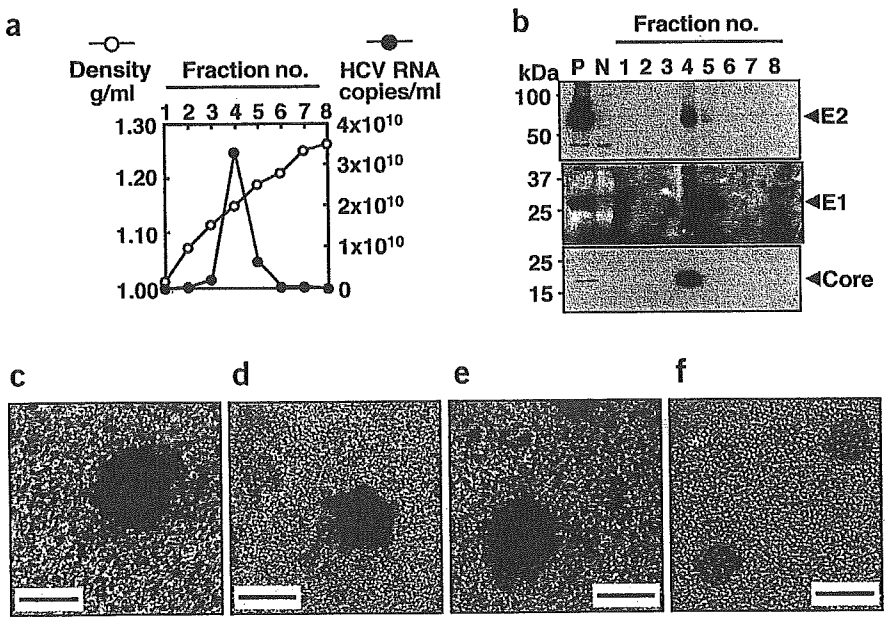

Figure 3 Density gradient and electron microscope analysis of recombinant HCV particles. (a,b) Co-sedimentation of viral RNA and structural proteins. (a) Concentrated culture medium collected from JFH1/E2HA RNA–transfected cells was fractionated using a 10–60% sucrose density gradient. HCV RNA titer in each fraction was determined. (b) Density gradient fractions were further concentrated and analyzed by western blotting for core, E1 or E2-hemagglutinin. P, cell lysate prepared from JFH1/E2HA RNA–transfected Huh7 cells; N, cell lysate from untransfected Huh7 cells. Arrowheads indicate positions of HCV proteins. (c–f) Electron micrograph of spherical structures shown by immunogold labeling. Grids were incubated with a concentrated JFH1 virus stock and then with the E2 monoclonal antibody CBH5 (ref. 14). Bound antibodies were detected with Protein A coupled to gold particles 10 nm in diameter. (c–e) Three representative examples showing the same structure. (f) Control grid coated with concentrated cell-free supernatant derived from mock-transfected cells. In rare cases, we observed gold particles attached to unstructured protein aggregates. Scale bar, 50 nm.

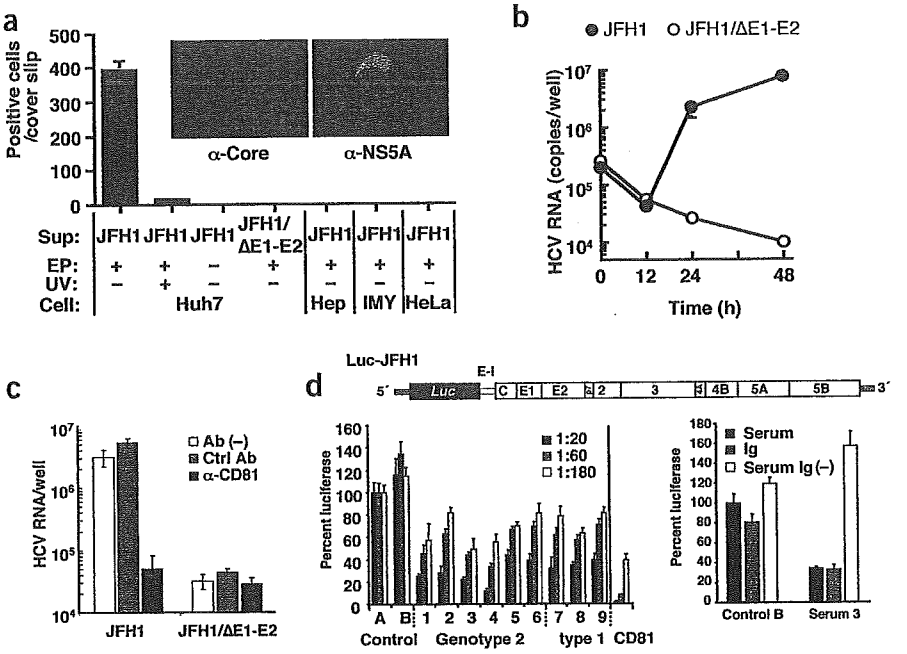

Figure 4 Infectivity of viral particles and neutralization of infection. (**a**, insert) Immunofluorescence analysis of cells infected with viral particles for core (left) and NS5A (right). (**a**) Cell lines specified on the bottom were also inoculated with a 1/30 concentrated supernatant from full-length JFH1 RNA– or JFH1/ΔE1-E2 RNA–transfected cells (Sup). In some experiments, culture supernatant of nontransfected cells was used (EP–), or culture supernatant was irradiated with ultraviolet light before inoculation of cells (UV+). (**b**) Comparison of infectivity of culture supernatant from JFH1 RNA– and JFH1/ΔE1-E2 RNA–transfected cells. (**c**) Inhibition of infection by CD81-specific antibody. We used 1/20 concentrated supernatants from cells transfected with given genomes for infection of Huh7 cells in the presence of a CD81-specific (α-CD81, black bars) or a control antibody (Ctrl Ab, gray bars), or in the absence of antibody (Ab(–), white bars). Inoculated cells were analyzed by RTD-PCR. (**d**) Production of infectious HCV particles carrying the firefly luciferase reporter gene and neutralization of infection by sera from infected individuals. Upper panel, schematic representation of Luc-JFH1 construct with luciferase (Luc) reporter gene (**Supplementary Fig. 6** online). E-I, EMCV-IRES. Bottom left panel, neutralization of Luc-JFH1 virus by sera from infected individuals. Luc-JFH1 viral particles were mixed with given dilutions of sera from healthy donor (Control), or sera from individuals infected with given genotypes (lanes 1–9). Results of CD81-specific antibody neutralization are shown in the right; black bar, 2 μg/ml; gray bar, 0.4 μg/ml; white bar, 0.08 μg/ml. Luciferase activity is expressed relative to the values obtained with control serum A. Bottom right panel, neutralization by immunoglobulins purified from infected individuals' sera. Luc-JFH1 virus particles were mixed with control serum B or patient serum 3 (serum, black bars), 2 mg protein of the same sera depleted of immunoglobulins (Serum Ig(–), open bars), or 130 μg of corresponding purified immunoglobulins (Ig, gray bars). Infectivity is expressed relative to control serum B.

(**Fig. 5**). We sequenced parts of the 5′-untranslated region (UTR; nucleotides 128–331), the E2 HVR (nucleotides 1,438–1,828) and NS5B (nucleotides 9,049–9,382) of the circulating viral RNA at week 4 after the last inoculation. The sequences were identical to the JFH1 strain. These results show the *in vivo* infectivity of JFH1 virus produced in culture.

DISCUSSION

This study shows that recombinant HCV particles are produced and secreted from JFH1 RNA–transfected cells, and secreted viruses are infectious for both Huh7 cells and a chimpanzee. Biochemical analyses show that cell culture–grown virus particles have a density of 1.15–1.17 g/ml and are spherical in size, with an average outer diameter of about 55 nm. Infectivity can be neutralized by CD81-specific antibodies, supporting the importance of CD81 in HCV entry[19,20]. Neutralization and cross-neutralization were achieved with immunoglobulins from infected individuals' sera. Cross-neutralization was also found with chimeric viruses composed of the core to NS2 region of the Con1 isolate (genotype 1) and the JFH1 replicase (T.P., G. Koutsoudakis, S. Kallis, T.K., T.W & R.B., unpublished data), indicating conserved epitopes involved in HCV entry. The possibility to create chimeric infectious virus broadens the scope of this system and allows (cross-)neutralization to be addressed in more detail.

It is unclear why the spread of infection in Huh7 cells is limited. Activation of innate immunity in transfected or infected cells is one possibility. Alternatively, JFH1 RNA–containing cells may have a growth disadvantage and therefore be displaced during passage. Moreover, formation of assembly-competent envelope protein complexes and virus release may be a rate-limiting step, reducing virus production to a level insufficient to sustain infection.

Earlier attempts to infect Huh7 cells with sera from infected individuals were not successful. But recombinant viral particles have a homogeneous density, whereas HCV in human sera shows much lower and heterogeneous densities, suggesting an association with cellular com-

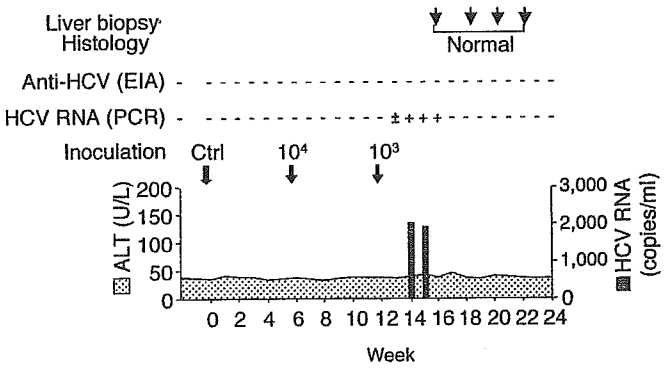

Figure 5 *In vivo* infectivity of JFH1 virus produced in tissue culture. Chimpanzee X0205 was first inoculated with 1 ml of the undiluted culture medium from mock-transfected Huh7 cells (Ctrl). We re-inoculated the chimpanzee 6 weeks later with 1 ml of a 10^4 dilution of culture medium from full-length JFH1 RNA-transfected cells (10^4). After 6 more weeks, we repeated inoculation with 1 ml of a 10^3 dilution (10^3). The course of infection is shown with arrows indicating the three inoculations. HCV RNA (copies/ml) and ALT (units/L) levels are plotted; HCV-specific, HCV RNA and liver biopsy results are shown above the graph.

ponents, especially lipoproteins[21], that may interfere with infection. Further studies are required to analyze the mechanism underlying the different infectivities of recombinant and serum-derived virus particles, especially using the serum from JFH1 virus–infected chimpanzee.

Culture-grown JFH1 viral particles are infectious in chimpanzee. The ratio of RNA titer versus infectious titer of the culture medium is about 1,000, which is lower than reported for infectious human and chimpanzee serum (10–100)[22,23]. Possible explanations are more defective viruses produced by the JFH1 strain or overestimation of viral RNA because of the input RNA used for transfection. Notably, human sera with lower infectivity have a density of about 1.17 g/ml, whereas those with higher infectivity sediment primarily at a lower density[24].

The transient course of infection of the JFH1 strain differs from most infectious clones[22,25,26], usually causing higher viremia and occasionally HCV-specific seroconversion or hepatocellular injury. This may result from the inoculum (culture grown virus versus inoculation of genomic *in vitro* transcripts) or the rather old age of the chimpanzee (20–30 years). Alternatively, the JFH1 strain, although replicating efficiently *in vitro*[8–10], may be less infectious *in vivo*[27]. Nevertheless, this is the first report describing the production of HCV in cell culture, which can infect both cells and primates.

METHODS

For details of Methods, please see **Supplementary Methods** *online.*

Plasmid construction. Based on the consensus sequence of JFH1 (ref. 7), we assembled plasmid pJFH1 containing the full-length JFH1 cDNA downstream of the T7 RNA promoter. We generated the following mutants of pJFH1: pJFH1/GND carrying a mutation in the NS5B GDD motif, which abolishes RNA polymerase activity[4,5]; pJFH1/ΔE1-E2 with a deletion of 351 amino acids (amino acids 217–567); pJFH1/E2HA with the hemagglutinin tag (YPYDVPDYA) replacing part of the E2 HVR (amino acids 394–402). pJ6CF is the prototype genotype 2a clone[11]. We constructed plasmid pJCH1 analogous to pJFH1 (ref. 7). In plasmid pFK-Luc-JFH1, the 5′-UTR and part of the core region were fused to the firefly luciferase gene. The second cistron is expressed through the encephalomyocarditis virus internal ribosomal entry site and encodes the complete JFH1 polyprotein.

RNA transfection and analysis of transfected cells. *In vitro* synthesis of HCV RNA, electroporation and northern blot analysis were performed as described previously[4,8]. For detection of HCV proteins by western blot, we used NS5A (ref. 9), NS3 (ref. 8) and core-specific (clone 2H9) antibodies and peroxidase-labeled rabbit-specific goat immunoglobulin (Biosource) or mouse-specific sheep immunoglobulin (Amersham Pharmacia). E1- and E2-specific polyclonal antibodies were raised by immunization of rabbits with synthetic peptides. We used rat monoclonal hemagglutinin-specific antibody (Roche) and peroxidase-labeled rat-specific goat IgG to detect hemagglutinin-tagged E2 protein. Immunofluorescence was performed using the same primary antibodies.

Quantification of HCV core protein and RNA. We quantified HCV core protein in culture supernatant or cell lysate using a new immunoassay described previously[28]. Total RNA was isolated from cell lysates or culture media by Isogen (Nippon Gene). We determined RNA copy numbers of HCV by RTD-PCR as described[12].

Sucrose density gradient analysis. We cleared culture medium collected 6 d after transfection using low-speed centrifugation, and passed it through a 0.45-μm filter. We layered filtrate on a sucrose gradient (60% to 10%, wt/vol) and centrifuged it for 16 h. We harvested and analyzed fractions for HCV RNA titers using RTD-PCR.

Infection of cells with secreted HCV. We collected culture medium 72 h after transfection, cleared it using low-speed centrifugation and passed it through a 0.45-μm filter. Part of the filtrate was concentrated 1/30 using an Amicon Ultra-15 (cut off: 1×10^5 Da; Millipore). We seeded cells 24 h before infection at a density of 5×10^4 cells/well in a 12-well plate, or at 1×10^5 cells/well in a 6-well plate. We infected cells with 100 μl of inoculum for 3 h, washed them, added complete medium and cultured cells for 12, 24, 48, 72 and 96 h. We performed immunofluorescence 2 d after infection.

Electron microscopy. We concentrated supernatant harvested from JFH1-transfected Huh7 cells and mock-transfected cells using ultracentrifugation and adsorbed it onto carbon-coated grids. Grids were fixed with 3% paraformaldehyde, and blocked in a solution of 0.8% BSA, 1% coldwater fish skin gelatin (Sigma) and 20 mM glycine. We performed immunogold labeling with an E2-specific antibody (CBH5) and Protein A coupled to 10-nm gold particles. After extensive washing, we stained grids with 1.8% methylcellulose and 0.3% uranyl acetate.

Virus neutralization assays. Target cells were infected with culture supernatants supplemented with JS-81 (BD Biosciences) or Mab46D2 (Dengue type 2–specific antibody) at a final concentration of 10 μg/ml (unless otherwise stated). After inoculation, we supplemented cells with fresh medium. We lysed cells 72 h after infection for RTD-PCR or luciferase assays.

For neutralization with sera from infected individuals, we mixed virus-containing supernatants with dilutions of heat-inactivated serum. After incubation for 1 h, we added mixtures to target cells and measured infection. Immunoglobulins contained in human sera were purified by using a HiTrap Affinity Protein G column (Amersham Pharmacia).

***In vivo* infection.** The chimpanzee experiment was conducted at Southwest Foundation for Biomedical Research (SFBR), San Antonio, Texas, in an American Association of Laboratory Animal Care–accredited animal facility under animal protocol approved by SFBR Institutional Animal Care and Use Committee. We collected culture medium from Huh7 cells transfected with the JFH1 genome and cleared them by centrifugation before inoculation into chimpanzee X0205. Serum samples were tested for alanine aminotransferase levels, HCV-specific antibodies (EIA2.0, Abbott Laboratories) and HCV RNA that was quantified by the Roche Amplicor Cobas Monitor II (Roche). We collected liver biopsies for histological analysis.

Accession numbers. The Genbank accession numbers for the consensus sequence of JFH1 is AB047639 and for JCH1 it is AB047640.

ACKNOWLEDGMENTS

This study was supported by a Grant-in-Aid for Scientific Research from the Japan Society for the Promotion of Science, by a Grant from Toray Industries, Inc., by the Program for Promotion of Fundamental Studies in Health Sciences of the Pharmaceuticals and Medical Devices Agency (PMDA), by the Research on Health Sciences focusing on Drug Innovation from the Japan Health Sciences Foundation, by the National Heart, Lung and Blood Institute contract N01-HB-27091 for the use of chimpanzees, by a grant from the European Community (QLK2-CT-2002-01329), and by a grant from the Deutsche Forschungsgemeinschaft (SFB 638; Teilprojekt A5). T.K. was partially supported by Hepatitis Virus Research Foundation of Japan. The authors are grateful to J. Bukh for providing the pJ6CF plasmid, to S. Foung for provision of the antibody CBH5, to S. Koike for his comments, to K. Yasui, S. Sone and J.-I. Tanabe for their support, to G. Koutsoudakis and E. Steinmann, and to S. Kallis and U. Herian for technical assistance. We are also grateful to K. Takagi, K. Hiramatsu and members of Central Clinical Laboratory in Nagoya City University Hospital, R. Sapp of the Liver Diseases Branch, H. McClure of the Southwest Foundation for Biomedical Research for their technical assistance, H. Barth, B. Bartosch, T. Baumert, J. Encke and C. Sarrazin for providing human sera.

COMPETING INTERESTS STATEMENT

The authors declare that they have no competing financial interests.

Received 22 March; accepted 29 April 2005
Published online at http://www.nature.com/naturemedicine/

1. Choo, Q.L. *et al.* Isolation of a cDNA clone derived from a blood-borne non-A non-B viral hepatitis genome. *Science* **244**, 359–362 (1989).
2. Kiyosawa, K. *et al.* Interrelationship of blood transfusion, non-A, non-B hepatitis and hepatocellular carcinoma: analysis by detection of antibody to hepatitis C virus. *Hepatology* **12**, 671–675 (1990).
3. Bartenschlager, R. & Lohmann, V. Replication of hepatitis C virus. *J. Gen. Virol.* **81**, 1631–1648 (2000).

4. Lohmann, V. *et al.* Replication of subgenomic hepatitis C virus RNAs in a hepatoma cell line. *Science* **285**, 110–113 (1999).
5. Ikeda, M., Yi, M., Li, K. & Lemon, S.M. Selectable subgenomic and genome-length dicistronic RNAs derived from an infectious molecular clone of the HCV-N strain of hepatitis C virus replicate efficiently in cultured Huh7 cells. *J. Virol.* **76**, 2997–3006 (2002).
6. Pietschmann, T. *et al.* Persistent and transient replication of full-length hepatitis C virus genomes in cell culture. *J. Virol.* **76**, 4008–4021 (2002).
7. Kato, T. *et al.* Sequence analysis of hepatitis C virus isolated from a fulminant hepatitis patient. *J. Med. Virol.* **64**, 334–339 (2001).
8. Kato, T. *et al.* Efficient replication of the genotype 2a hepatitis C virus subgenomic replicon. *Gastroenterology* **125**, 1808–1817 (2003).
9. Date, T. *et al.* Genotype 2a hepatitis C virus subgenomic replicon can replicate in HepG2 and IMY-N9 cells. *J. Biol. Chem.* **279**, 22371–22376 (2004).
10. Kato, T. *et al.* Non-hepatic cell lines HeLa and 293 cells support efficient replication of hepatitis C virus genotype 2a subgenomic replicon. *J. Virol.* **79**, 592–596 (2005).
11. Yanagi, M., Purcell, R.H., Emerson, S.U. & Bukh, J. Hepatitis C virus: an infectious molecular clone of a second major genotype (2a) and lack of viability of intertypic 1a and 2a chimeras. *Virology* **262**, 250–263 (1999).
12. Takeuchi, T. *et al.* Real-time detection system for quantification of hepatitis C virus genome. *Gastroenterology* **116**, 636–642 (1999).
13. Forns, X. *et al.* Hepatitis C virus lacking the hypervariable region 1 of the second envelope protein is infectious and causes acute resolving or persistent infection in chimpanzees. *Proc. Natl Acad. Sci. USA* **97**, 13318–13323 (2000).
14. Hadlock, K.G. *et al.* Human monoclonal antibodies that inhibit binding of hepatitis C virus E2 protein to CD81 and recognize conserved conformational epitopes. *J. Virol.* **74**, 10407–10416 (2000).
15. Takahashi, K. *et al.* p26 protein and 33-nm particle associated with nucleocapsid of hepatitis C virus recovered from the circulation of infected hosts. *Virology* **191**, 431–434 (1992).
16. He, L.F. *et al.* Determining the size of non-A, non-B hepatitis virus by filtration. *J. Infect. Dis.* **156**, 636–640 (1987).
17. Kaito, M. *et al.* Hepatitis C virus particle detected by immunoelectron microscopic study. *J. Gen. Virol.* **75**, 1755–1760 (1994).
18. Shimizu, Y.K., Feinstone, S.M., Kohara, M., Purcell, R.H. & Yoshikura, H. Hepatitis C virus: Detection of intracellular virus particles by electron microscopy. *Hepatology* **23**, 205–209 (1996).
19. Bartosch, B., Dubuisson, J. & Cosset, F.L. Infectious hepatitis C virus pseudo-particles containing functional E1–E2 envelope protein complexes. *J. Exp. Med.* **197**, 633–642 (2003).
20. Hsu, M. *et al.* Hepatitis C virus glycoproteins mediate pH-dependent cell entry of pseudotyped retroviral particles. *Proc. Natl Acad. Sci. USA* **100**, 7271–7276 (2003).
21. Thomssen, R. *et al.* Association of hepatitis C virus in human sera with beta-lipoprotein. *Med. Microbiol. Immunol. (Berl.)* **181**, 293–300 (1992).
22. Thomson, M. *et al.* The clearance of hepatitis C virus infection in chimpanzees may not necessarily correlate with the appearance of acquired immunity. *J. Virol.* **77**, 862–870 (2003).
23. Major, M.E. *et al.* Previously infected and recovered chimpanzees exhibit rapid responses that control hepatitis C virus replication upon rechallenge. *J. Virol.* **76**, 6586–6595 (2002).
24. Hijikata, M. *et al.* Equilibrium centrifugation studies of hepatitis C virus: evidence for circulating immune complexes. *J. Virol.* **67**, 1953–1958 (1993).
25. Kolykhalov, A.A. *et al.* Transmission of hepatitis C by intrahepatic inoculation with transcribed RNA. *Science* **277**, 570–574 (1997).
26. Yanagi, M., Purcell, R.H., Emerson, S.U. & Bukh, J. Transcripts from a single full-length cDNA clone of hepatitis C virus are infectious when directly transfected into the liver of a chimpanzee. *Proc. Natl Acad. Sci. USA* **94**, 8738–8743 (1997).
27. Bukh, J. *et al.* Mutations that permit efficient replication of hepatitis C virus RNA in Huh-7 cells prevent productive replication in chimpanzees. *Proc. Natl Acad. Sci. USA* **99**, 14416–14421 (2002).
28. Aoyagi, K. *et al.* Development of a simple and highly sensitive enzyme immunoassay for hepatitis C virus core antigen. *J. Clin. Microbiol.* **37**, 1802–1808 (1999).
29. Kato, T. *et al.* Processing of hepatitis C virus core protein is regulated by its C-terminal sequence. *J. Med. Virol.* **69**, 357–366 (2003).

Journal of General Virology (2005), 86, 2209–2220 DOI 10.1099/vir.0.80638-0

Characterization of the E-138 (Glu/Lys) mutation in *Japanese encephalitis virus* by using a stable, full-length, infectious cDNA clone

Zijiang Zhao,[1] Tomoko Date,[1] Yuhua Li,[2] Takanobu Kato,[1] Michiko Miyamoto,[1] Kotaro Yasui[1] and Takaji Wakita[1]

[1]Department of Microbiology, Tokyo Metropolitan Institute for Neuroscience, 2-6 Musashidai, Fuchu-shi, Tokyo 183-8526, Japan

[2]Chengdu Institute of Biological Products, Chengdu 610063, Sichuan Province, PR China

Correspondence
Takaji Wakita
wakita@tmin.ac.jp

Received 25 September 2004
Accepted 21 April 2005

A stable plasmid DNA, pMWJEAT, was constructed by using full-length *Japanese encephalitis virus* (JEV) cDNA isolated from the wild-type strain JEV AT31. Recombinant JEV was obtained by synthetic RNA transfection into Vero cells and designated rAT virus. JEV rAT exhibited similar large-plaque morphology and antigenicity to the parental AT31 strain. Mutant clone pMWJEAT-E138K, containing a single Glu-to-Lys mutation at aa 138 of the envelope (E) protein, was also constructed to analyse the mechanisms of viral attenuation arising from this mutation. Recombinant JEV rAT-E138K was also recovered and displayed a smaller-plaque morphology and lower neurovirulence and neuroinvasiveness than either AT31 virus or rAT virus. JEV rAT-E138K exhibited greater plaque formation than rAT virus in virus–cell interactions under acidic conditions. Heparin or heparinase III treatment inhibited binding to Vero cells more efficiently for JEV rAT-E138K than for rAT virus. Inhibition of virus–cell interactions by using wheatgerm agglutinin was more effective for JEV rAT than for rAT-E138K on Vero cells. About 20 % of macropinoendocytosis of JEV rAT for Vero cells was inhibited by cytochalasin D treatment, but no such inhibition occurred for rAT-E138K virus. Furthermore, JEV rAT was predominantly secreted from infected cells, whereas rAT-E138K was more likely to be retained in infected cells. This study demonstrates clearly that a single Glu-to-Lys mutation at aa 138 of the envelope protein affects multiple steps of the viral life cycle. These multiple changes may induce substantial attenuation of JEV.

INTRODUCTION

Japanese encephalitis virus (JEV) belongs to the genus *Flavivirus*, which predominantly comprises arthropod-borne viruses. Members of this genus are distributed throughout the world. JEV has a single-strand, positive-sense RNA genome of approximately 11 000 nt, which is translated from a single open reading frame into a polyprotein that is processed by viral and host proteases to yield three structural proteins [capsid, membrane or precursor membrane (prM) and envelope (E)] encoded at the 5′ end of the genome, followed by at least seven non-structural proteins (Monath & Heinz, 1996). The flavivirus E protein is the viral haemagglutinin, which induces protective immunity and mediates receptor-specific virus attachment to cell surfaces (Kimura-Kuroda & Yasui, 1983). The E protein plays major roles in determining viral pathogenicity by defining cellular tropism and affecting penetration into susceptible cells (Heinz, 1986; Mandl *et al.*, 1989). X-ray crystallographic resolution of the structure of the E ectodomain in *Tick-borne encephalitis virus* (TBE virus) reveals that the E protein forms head-to-tail homodimers that lie parallel to the viral envelope (Rey *et al.*, 1995). These homodimers dissociate, leading to irreversible formation of homotrimers on the surface of viral particles under conditions of low pH (Allison *et al.*, 1995; Kuhn *et al.*, 2002; Stiasny *et al.*, 2002).

Studies attempting to elucidate the molecular basis of JEV attenuation have analysed the genomes of both the virulent parental strain SA14 and the attenuated vaccine virus SA14-14-2 (Nitayaphan *et al.*, 1990; Aihara *et al.*, 1991). Several JEV mutants have been obtained through γ-ray irradiation (Chen *et al.*, 1996) or passage in cultured cells (Hasegawa *et al.*, 1992). These studies have indicated that some mutations in the E protein correlate with viral attenuation, including the amino acid mutation from glutamic acid (Glu) to lysine (Lys) at residue 138 of the E protein (E-138). Due to the multiple mutations present, the

The GenBank/EMBL/DDBJ accession numbers for the sequences described in this study are given in Table 1.

Supplementary figures and tables are available in JGV Online.

exact mutated residue changes in the E protein that are primarily responsible for JEV attenuation are not clearly understood. Since infectious *Yellow fever virus* RNA was transcribed successfully from a full-length cDNA template by using *in vitro* ligation of two cDNA fragments (Rice *et al.*, 1989), infectious flavivirus clones have been constructed in similar fashion for JEV (Sumiyoshi *et al.*, 1992), dengue virus type 2 (Polo *et al.*, 1997; Gualano *et al.*, 1998), dengue virus type 4 (Lai *et al.*, 1991) and other viruses (Khromykh & Westaway, 1994; Gritsun & Gould, 1998; Shi *et al.*, 2002; Hayasaka *et al.*, 2004). This method seems valuable in studying biological function, polyprotein processing and virulence of mutant viruses with specific mutations in various regions of the viral genome. However, irregular mutations occur frequently in full-length JEV cDNA clones during cloning into plasmid vectors, particularly in the 5′ fragment, and this has seriously affected such studies (Sumiyoshi *et al.*, 1995; Yamshchikov *et al.*, 2001). Specific strategies are thus necessary to establish stable, full-length JEV infectious clones, such as insertion of short introns or cloning into bacterial artificial chromosomes (Yamshchikov *et al.*, 2001; Yun *et al.*, 2003).

The present report describes the construction of a stable, full-length cDNA clone of the wild-type JEV AT31 strain into the very low-copy-number plasmid pMW118 by using conventional molecular-cloning technology. Another plasmid, containing a Glu-to-Lys mutation at the E-138 residue, was also constructed. Recombinant JEVs comprising wild-type and mutant viruses were recovered after synthetic RNA transfection, and were characterized with regard to viral virulence, internalization and release.

METHODS

Cells, viruses, antibodies and mice. Vero cells and C6/36 cells were maintained in Eagle's minimum essential medium (MEM) supplemented with 5% fetal calf serum (FCS). Primary neural cells from cerebral cortices of embryonic BALB/c mice at gestational day 18 (Japan SLC) were maintained as described previously (Wilcox *et al.*, 1990).

The wild-type JEV strain AT31 was a gift from Dr Nakamura of the Nippon Institute for Biological Science, Japan. Attenuated JEV at222 strain was obtained after 222 passages through primary hamster kidney cells to obtain a vaccine strain, as described previously (Yasui, 2002). Recombinant wild-type rAT virus and mutant rAT-E138K were obtained from supernatants of Vero cells transfected with *in vitro*-transcribed RNAs. All cDNA sequences of viral RNAs were determined and deposited in GenBank/DDBJ/EMBL (Table 1). The at222 strain contains several mutations, including the Glu-to-Lys mutation at residue E-138. All viruses were propagated once in Vero cells or C6/36 cells and supernatants were obtained and stored at −80 °C until used. Three-day-old BALB/c mice were inoculated intracerebrally with 10^4 p.f.u. JEV rAT-E138K. The inoculated mice were sacrificed at 8 days of age and their brains were harvested and homogenized. Reverted virus RE-138 was recovered from a single large plaque on Vero cells inoculated with the supernatant of homogenized brains. Rabbit anti-JEV serum was prepared as described previously (Kimura-Kuroda *et al.*, 1993).

BALB/c mice were purchased from Japan SLC Inc. All mice were maintained in pathogen-free environments. All experiments were conducted in accordance with the Guidelines for the Care and Use of Animals, 2000 (Tokyo Metropolitan Institute for Neuroscience, Tokyo, Japan).

Construction of full-length cDNA and a point-mutant cDNA of JEV strain AT31. RNA was extracted from the supernatant of C6/36 cells infected with AT31 by using Isogen-LS (Nippon Gene). Oligonucleotide primers were designed based on sequence data for JEV strain JaOArS982 (GenBank/EMBL/DDBJ accession no. M18370; Sumiyoshi *et al.*, 1987) and the sequences of these primers are listed in Supplementary Table S1 (available in JGV Online). The RNA solution was subjected to reverse transcription (RT) using an antisense primer, JEV-10976R-30, and Moloney murine leukemia virus reverse transcriptase (Superscript II; Invitrogen) at 42 °C for 1 h. Both 5′ and 3′ fragments of JEV cDNA (nt 1–6125 and 5383–10976, respectively) were amplified by using two pairs of primers: SalT7GJE5P20S and JEV-6125R-30 for the 5′ fragment or JEV-5383S-30 and ClaKpnJE3P30R for the 3′ fragment, with TaKaRa LA *Taq* polymerase. PCR conditions comprised 30 cycles of denaturing

Table 1. Origin, sequence, neurovirulence and neuroinvasiveness of JEV in this study

NA, Not applicable; ND, not done.

Virus	Origin	Sequence accession no.*	Neurovirulence† ($p.f.u./LD_{50}$)	Neuroinvasiveness‡ ($p.f.u./LD_{50}$)
AT31	Parent	AB196923	2·2	18 800
at222	Vaccine	AB196924	148 000	$>10^7$
rAT§	Recombinant‖	AB196925	2·5	24 200
rAT-E138K¶	Recombinant‖	AB196926	15 200	$>10^7$
RE-138	Reverted	NA	2·2	ND

*Sequences in GenBank/DDBJ/EMBL.
†Intracerebral inoculation with 0·025 ml virus solution in 3-week-old female BALB/c mice.
‡Intraperitoneal inoculation with 0·1 ml virus solution in 3-week-old female BALB/c mice.
§Transcribed RNA prepared from pMWJEAT.
‖Recombinant virus obtained by RNA transfection.
¶Transcribed RNA prepared from pMWJEAT-E138K.

at 95 °C for 10 s and annealing and extension at 68 °C for 6 min. PCR products containing 5′ and 3′ fragments of JEV cDNA were cloned into pBR322. Three cloned plasmids were selected for further reconstruction of a full-length JEV cDNA: pJEAT-5′-132 contained the 5′ end to the *Sac*I site (nt 2215) region; pJEAT-5′-258 contained the *Sac*I site (nt 2215) to *Bam*HI site (nt 5576) region; and pJEAT-3′-75 contained the *Bam*HI site (nt 5576) to 3′ end region (see Supplementary Fig. S1, available in JGV Online). For subcloning purposes, the second *Sac*I site in JEV cDNA was abolished by using PCR-based mutagenesis (Kato *et al.*, 2003a), with an A-to-T mutation at nt 6713 of pJEAT-3′-75, producing pJEAT-3′-75dSac. Each insert from pJEAT-5′-132, pJEAT-5′-258 and pJEAT-3′-75dSac was cloned stably into a very low-copy-number plasmid vector, pMW118 (Nippon Gene), to construct the full-length JEV cDNA and the result was designated pMWJEAT (see Supplementary Fig. S1, available in JGV Online). A single G-to-A point mutation at nt 1389 was also introduced into pMWJEAT by PCR-based mutagenesis and designated pMWJEAT-E138K (Fig. 1a).

Transfection of synthetic JEV RNA into Vero cells by electroporation. Plasmid DNAs pMWJEAT and pMWJEAT-E138K were digested by using *Kpn*I. JEV RNA was synthesized by using a MEGAscript T7 kit (Ambion) and treated with DNase I (RQ1 RNase-free DNase; Promega) followed by acid–phenol extraction (Kato *et al.*, 2003b). Trypsinized Vero cells were washed by using Opti-MEM I (Invitrogen) and resuspended in Cytomix buffer at $7{\cdot}5 \times 10^6$ cells ml^{-1} (Kato *et al.*, 2003b). Synthesized RNA (10 μg) mixed with 400 μl cell suspension was pulsed at 260 V and 950 μF by using a Gene Pulser II apparatus (Bio-Rad).

Plaque-reduction neutralization (PRNT) test. The PRNT test was done as described previously (Zhao *et al.*, 2003). PRNT titre was expressed as the maximum dilution of antibody yielding a 90 % reduction in viral infectivity ($PRNT_{90}$).

Mouse experiments. Groups of 3-week-old female BALB/c mice ($n=5$) were inoculated intracerebrally with 25 μl of a tenfold serially diluted virus solution (AT31, at222, rAT, rAT-E138K and RE-138). Similar groups of mice were inoculated intraperitoneally with 0·1 ml of a tenfold serially diluted virus solution. Mice were observed for 3 weeks after inoculation. End points of neurovirulence and neuroinvasiveness were identified as both mortality ratios and mean survival times. The LD_{50} was determined for each virus (Reed & Muench, 1938).

Groups of 3-week-old female BALB/c mice ($n=30$) were inoculated with 10^5 p.f.u. rAT in 25 μl or 10^7 p.f.u. rAT-E138K in 25 μl into the left footpad. At 2-day intervals after inoculation, two mice from each group were bled periorbitally before cardiac perfusion with HBSS solution (Invitrogen). Brains, livers, spleens and kidneys of mice were harvested. Tissue suspensions of 10 % (w/v) were prepared by using PBS, then homogenized immediately. After three cycles of freezing and thawing, these 10 % (w/v) tissue suspensions were centrifuged at 20 000 *g* at 4 °C for 1 h, then filtered through a 0·2 μm filter. Virus titres in filtered supernatant were determined by plaque assay on Vero cells.

Acid resistance of early virus–cell interactions. Vero cells (1×10^5) cultured in a six-well tissue-culture plate (Corning) were washed and pre-chilled at 4 °C for 2 h. After inoculation with 400 p.f.u. virus (m.o.i., 0·004 p.f.u. per cell) at 4 °C for 2 h,

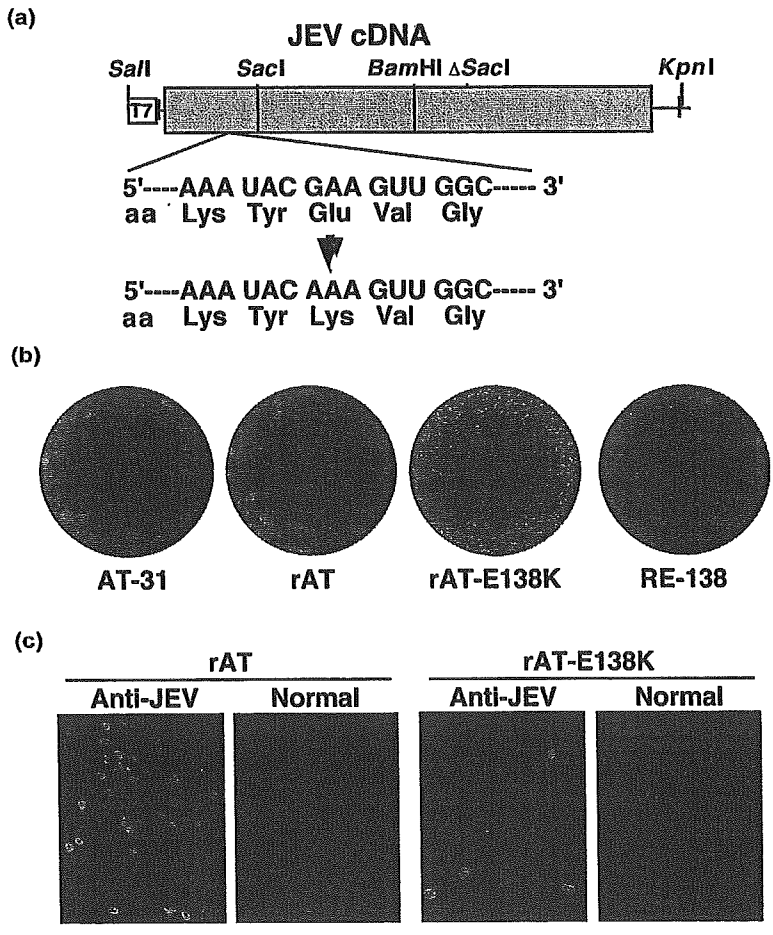

Fig. 1. (a) Schematic representation of the single point mutation in the full-length cDNA pMWJEAT-E138K of JEV AT31 strain, designated rAT-E138K strain. (b) Plaque morphology of wild-type virus AT31, recombinant virus rAT, mutant virus rAT-E138K and reverted virus RE-138. Vero cells infected with virus were fixed in 10 % formalin/PBS solution and stained by using 0·1 % crystal violet solution. (c) Detection of recombinant JEV rAT and rAT-E138K in the cerebral cortex of 3-week-old female BALB/c mice by using IFA, as described in Methods. Positive signals were observed in neuron-like cells in the cerebral cortex of rAT- and rAT-E138K-infected mice.

unbound virus was removed by washing three times with ice-cold MEM supplemented with 2% FCS (MEM-2). Cells were treated with 2 ml glycine/HCl-buffered saline (8 g NaCl, 0·38 g KCl, 0·10 g $MgCl_2.6H_2O$, 0·10 g $CaCl_2.2H_2O$ and 7·5 g glycine l^{-1}, pH adjusted to 3·0 with HCl) at room temperature for 5 min, as described by Hung *et al.* (1999), then overlaid with 1·25% methyl cellulose/MEM for incubation at 37 °C for 5 days. Infected cells without acid treatment were used as controls. Penetration rates of acid-resistant intracellular viruses were calculated as 100× [no. plaques (acid-treated)/no. plaques (controls)].

Heparin assay and heparinase-treatment effect on Vero cells. Inhibition of JEV binding to Vero cells by heparin (Sigma) was performed as described by Hung *et al.* (1999), with some modifications. The following two conditions were tested: (i) 400 p.f.u. virus plus heparin was pre-incubated at 37 °C for 1 h, then incubated in Vero cells cultured in a six-well plate at 37 °C for 2 h; and (ii) in total, 400 p.f.u. virus was reacted with heparin at 37 °C for 1 h, then inoculated into Vero cells at 4 °C for 2 h. Unbound virus was removed by three washes with MEM-2. Cells were overlaid with 1·25% methyl cellulose/MEM to incubate at 37 °C for 5 days. Cells inoculated by using the same procedure without heparin were used as controls. Inhibition was described as: 100× [no. plaques (heparin treatment)/no. plaques (controls)].

The effectiveness of heparinase treatment was analysed on Vero cells that had been treated with different concentrations of heparinase I or III (Sigma Aldrich) at 37 °C for 1 h. Cells cultured in a six-well plate were pre-chilled at 4 °C for 1 h after washing and inoculated with 400 p.f.u. per well (m.o.i., 0·004 p.f.u. per cell) of JEV rAT or rAT-E138K at 4 °C for 2 h. After washing in MEM-2, cells were overlaid with methyl cellulose and incubated at 37 °C for 5 days. Cells not treated with heparinase were used as controls. Inhibition was calculated as described above.

Binding inhibition of recombinant JEV with lectins. The ability of rAT and rAT-E138K to bind to Vero cells was examined by using concanavalin A (ConA; Sigma), wheatgerm agglutinin (WGA; Sigma) and phytohaemagglutinin P (PHA-P; Sigma) as described by Hung *et al.* (1999). A total of 400 p.f.u. virus was reacted with lectin at 37 °C for 1 h, then inoculated into Vero cells cultured in a six-well plate for 2 h. After washing in MEM-2, cells were overlaid with methyl cellulose and incubated at 37 °C for 5 days. Cells inoculated by using viral solutions without lectin were used as controls. Inhibition was calculated as: 100× [no. plaques (lectin treatment)/no. plaques (controls)].

Endocytosis inhibition. Inhibition of rAT and rAT-E138K virus internalization into Vero cells was analysed by using different concentrations of chlorpromazine, cytochalasin D or nystatin (all from Sigma). Vero cells cultured in a six-well plate were treated with these reagents at 37 °C for 1·5 h. These cells were subsequently inoculated with 400 p.f.u. JEV at 37 °C for another 3 h in the presence of the reagents, followed by treatment with glycine/HCl-buffered saline at room temperature for 5 min to inactivate unpenetrated viruses on the cell surface. Inoculated cells without any inhibiting agent were used as controls. Inhibition was calculated as: 100× [no. plaques (agent treatment)/no. plaques (controls)].

Immunohistochemistry. BALB/c mice (3 weeks old; $n=5$) received inoculation with 10 p.f.u. JEV rAT or 10^5 p.f.u. rAT-E138K into the right cerebral hemisphere. Virus titres were detected in the right hemispheres of sacrificed moribund mice. Left hemispheres were embedded immediately in Tissue-Tek embedding medium (Sakura Finetechnical) to examine the presence of JEV antigen with rabbit anti-JEV serum by using an immunofluorescence assay (IFA) as described previously (Zhao *et al.*, 2003).

Statistical analysis. Statistical analysis was performed by using Student's *t*-test. Survival rates of inoculated mice were analysed by using Kaplan–Meier methods. Values of $P<0·05$ were considered statistically significant.

RESULTS

Construction of a single plasmid DNA containing full-length JEV cDNA

Cloning a full-length JEV cDNA into a single plasmid vector, such as pUC or even a low-copy-number plasmid vector like pBR322 (Sumiyoshi *et al.*, 1992), is difficult without the insertion of short introns (Yamshchikov *et al.*, 2001). We thought that this difficulty might be attributable to toxicity of the proteins produced by JEV cDNA in transformed bacterial cells. To reduce this toxicity, we cloned full-length JEV cDNA into the very low-copy-number vector pMW118, a derivative of pSC101 (see Supplementary Fig. S1, available in JGV Online). The resultant plasmid, pMWJEAT, contained a full-length cDNA of the JEV AT31 strain and was amplified stably in bacterial cells. A mutant plasmid, pMWJEAT-E138K, containing a single Glu-to-Lys point mutation at aa 138 of the E protein, was also constructed (Fig. 1a).

Generation of recombinant JEV on Vero and C6/36 cells

The cDNA-generated recombinant JEV strains rAT and rAT-E138K were obtained from the supernatant of Vero cells transfected with synthetic RNA using the full-length cDNA clone as described in Methods. Viral RNA was extracted from both rAT and rAT-E138K virus solutions and sequences were determined directly after RT-PCR. No mutations were found in the genomic sequences as compared with template plasmid DNA sequences. Parental wild-type AT31 and recombinant rAT viruses displayed similar plaque morphologies at 5 days after infection (diameter ~3·1 mm), whereas rAT-E138K virus exhibited a smaller-plaque morphology (diameter ~0·45 mm) on Vero cells (Fig. 1b). Plaques similar to those of rAT-E138K were observed in all supernatant samples following seven passages on C6/36 cells. Reverted RE-138 virus was obtained as described in Methods. RE-138 virus also exhibited larger-size plaques (~3·1 mm) than those of AT31 and rAT viruses, as shown in Fig. 1(b).

Neurovirulence and neuroinvasiveness of recombinant JEV

Neurovirulence and neuroinvasiveness of JEV strains were determined by direct intracerebral inoculation or intraperitoneal infection using the tested viruses obtained from the supernatants of infected cells, as described in Methods. The JEV rAT strain displayed strong neurovirulence in 3-week-old BALB/c mice, as did the parent AT31 (2·5 and 2·2 p.f.u./LD_{50}, respectively; Table 1). In contrast, the rAT-E138K strain displayed much lower neurovirulence in mice

(15 200 p.f.u./LD_{50}) and the attenuated JEV at222 strain displayed the lowest neurovirulence (148 000 p.f.u./LD_{50}). However, RE-138 virus reverted from the rAT-E138K strain displayed strong neurovirulence (2·2 p.f.u./LD_{50}; Table 1), comparable to that seen with rAT and AT31 virus. After sequence analysis of RE-138 virus from the supernatant of infected Vero cells, only residue E-138 had been changed from Lys to Glu, compared with the rAT-E138K virus (data not shown). Furthermore, the JEV rAT strain demonstrated strong neuroinvasiveness, comparable to that of the parental AT31 strain (18 800 and 24 200 p.f.u./LD_{50}, respectively). Both rAT-E138K and at222 strains exhibited weak neuroinvasiveness ($>10^7$ p.f.u./LD_{50} for both strains), as all mice inoculated with 10^7 p.f.u. of either rAT-E138K or at222 survived (Table 1). These results demonstrate that the Glu-to-Lys mutation at residue E-138 of the JEV AT31 strain strongly attenuates viral neurovirulence and neuroinvasiveness in BALB/c mice.

Detection of JEV antigen in inoculated mouse brain

Positive signals were detected in both rAT- and rAT-E138K-infected mouse brains by IFA, and most positive cells displayed a neuronal morphology (Fig. 1c). The majority of positive signals were distributed in both the cerebral cortex and putaminal areas in brains of rAT-infected mice, whereas most positive cells were present in the frontal area of the cerebral cortex in rAT-E138K-infected mice. No positive signals were identified in the cerebella of either rAT- or rAT-E138K-infected mice (data not shown). These results indicate that the point mutation does not change viral neurotropism in BALB/c mice, although neurovirulence is attenuated.

JEV titre of infected mouse tissues

All mice inoculated with 10^7 p.f.u. rAT-E138K into the left footpad remained asymptomatic until 14 days post-inoculation, and no virus replication was detected in any tested tissue (Table 2). In contrast, viraemia (163 p.f.u. ml^{-1}) was detected in sera of mice inoculated with 10^5 p.f.u. of the rAT strain via the footpad on day 2 post-inoculation. Detectable levels of replicated rAT virus in brains of inoculated mice were identified at about $1·2 \times 10^4$ p.f.u. per tissue at 4 days post-inoculation, increasing to $8·6 \times 10^7$ p.f.u. per tissue by day 8. No virus was detected in any other tissue (Table 2).

Alteration in acid-resistant viral attachment by Glu-to-Lys mutation at E-138

Some flaviviruses display abolished infectivity with low-pH treatment after adsorption onto target cells (Hung *et al.*, 1999). We thus attached JEVs to Vero cells at 4 °C and then created conditions of low pH to determine the extent to which the adsorbed virus can maintain infectivity. Substantial reduction in plaque formation was detected in the rAT strain under conditions of low pH, with 7·79±2·31 % plaque formation compared with the control experiment (Fig. 2). However, rAT-E138K and at222 strains proved more resistant to low-pH treatment, with plaque formation at 35·95±9·61 and 34·83±4·19 %, respectively. These results indicate that the Glu-to-Lys mutation at E-138 alters the acid resistance of virus–cell attachment on Vero cells.

Table 2. Organ distribution of JEV in 3-week-old BALB/c mice inoculated with either 1×10^5 p.f.u. rAT or 1×10^7 p.f.u. rAT-E138K via the footpad

Virus	Virus titres in organ*				
	Serum	Brain	Kidney	Liver	Spleen
rAT					
0 d.p.i.†	−‡	−‡	−	−	−
2 d.p.i.	163	−	−	−	−
4 d.p.i.	−	$1·2 \times 10^4$	−	−	−
6 d.p.i.	−	$4·3 \times 10^7$	−	−	−
8 d.p.i.§	−	$8·6 \times 10^7$	−	−	−
rAT-E138K‖					
0 d.p.i.	−	−	−	−	−
14 d.p.i.	−	−	−	−	−

*Virus titre measured as p.f.u. ml^{-1} for serum, or p.f.u. per tissue for tissues.
†d.p.i., Days post-inoculation.
‡Virus titre, <25 p.f.u. ml^{-1} or <25 p.f.u. per tissue.
§Mice inoculated with 1×10^5 p.f.u. rAT were sacrificed at 8 days post-inoculation.
‖All mice inoculated with 1×10^7 p.f.u. rAT-E138K survived and no detectable virus (<25 p.f.u.) was identified in any tissues of mice sacrificed at 2-day intervals up to 14 days post-inoculation. Negative results at other days are not shown.

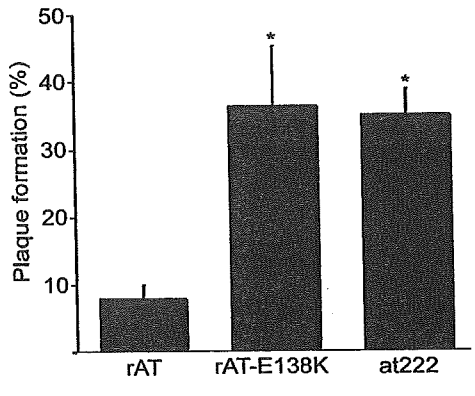

Fig. 2. Virus–cell interactions for recombinant JEV on Vero cells. Plaque-formation rates of rAT, rAT-E138K and attenuated at222 viruses bound to Vero cells at 4 °C were examined following treatment with glycine/HCl-buffered saline (pH 3·0) at room temperature for 5 min. Each value represents the mean of nine wells from three separate experiments. Error bars indicate SD. *, $P<0·01$.

Inhibition of virus–cell interactions with heparin or heparinase treatment

Both heparin and heparinase treatments have been used to inhibit the interactions of flavivirus and target cells (Chen *et al.*, 1997; Hung *et al.*, 1999). Infection by the rAT-E138K strain was clearly inhibited by heparin on Vero cells, whereas the rAT strain remained unaffected at both 4 and 37 °C (Fig. 3a, b). Significant differences in heparin inhibition between rAT and rAT-E138K were detected with heparin concentrations of 0·1–100 U ml^{-1} at 37 °C ($P<0·01$ or $P<0·001$; Fig. 3a) and of 0·1–1000 U ml^{-1} at 4 °C ($P<0·05$, $P<0·01$ or $P<0·001$; Fig. 3b), respectively. Similar results were noted on addition of heparin after virus attachment to Vero cells (data not shown).

Next, heparan sulphate on the surface of Vero cells was eliminated by treatment with heparinase I or III. Plaque formation for the JEV rAT strain on Vero cells was not inhibited by heparinase I or III treatment (Fig. 3c, d). However, plaque formation by rAT-E138K virus was reduced by both heparinase I and III (Fig. 3c, d). Differences in the plaque formation of infected Vero cells treated with heparinase I were small ($P<0·05$ at 4 U ml^{-1}; Fig. 3c). Treatment with >1 U heparinase III ml^{-1} on Vero cells reduced plaque formation of rAT-E138K by >40 %, but had no effect on rAT virus, representing a significant difference ($P<0·001$ for approx. 1–4 U heparinase III ml^{-1}; Fig. 3d). These data demonstrate that the point mutation increases dependency on heparan sulphate B residues for virus attachment to the cell surface.

Inhibition of virus–cell interactions with lectins

Regulation of viral entry by carbohydrates on dengue virus type 2 glycoproteins has been reported (Hung *et al.*, 1999). To explore the effect of the point mutation in JEV

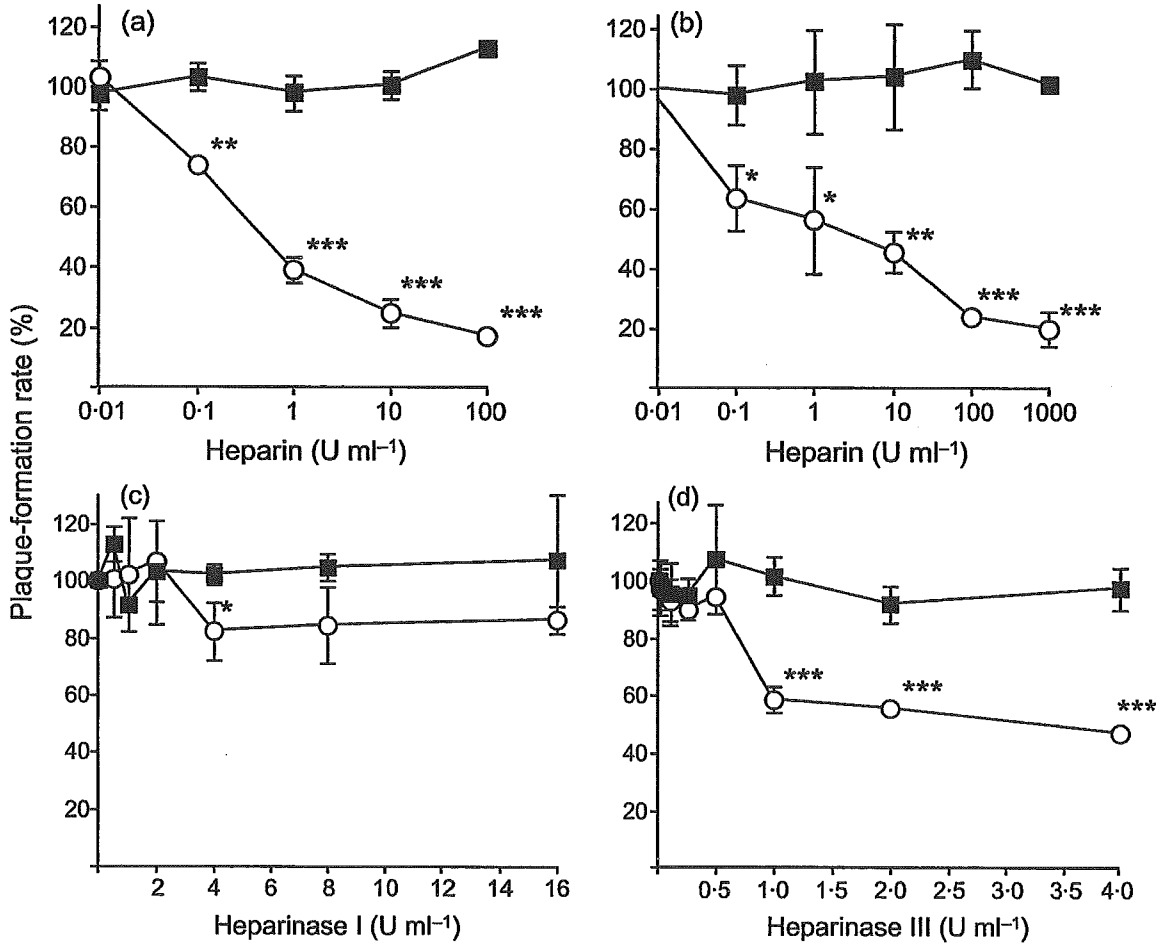

Fig. 3. Inhibition of recombinant JEV rAT (■) and rAT-E138K (○) plaque formation on Vero cells with heparan sulphate were analysed at 37 °C (a) and 4 °C (b). Plaque-formation rates of rAT (■) and rAT-E138K (○) viruses on Vero cells treated with heparinase I (c) or heparinase III (d) at 37 °C for 1 h were examined. Each value represents the mean of nine wells from three separate experiments. Error bars indicate SD. *, $P<0·05$; **, $P<0·01$; ***, $P<0·001$.

glycoproteins on this regulation, various lectins were used to inhibit virus–cell interactions. No significant differences in plaque formation were seen following ConA treatment between JEV rAT and rAT-E138K strain infection on Vero cells (Fig. 4a). However, significant differences in plaque formation were found between rAT and rAT-E138K strains when virus was treated with >5 μg WGA ml^{-1} pre-inoculation ($P<0{\cdot}01$ or $P<0{\cdot}001$; Fig. 4b). Finally, PHA-P did not reduce plaque formation in either JEV rAT or rAT-E138K strains at any tested concentration (Fig. 4c). These results indicate that the point mutation affects inhibition of virus–cell interactions with WGA, but exerts less effect with ConA and PHA-P. The higher efficiency of WGA inhibition against the rAT strain than against the rAT-E138K strain suggests that residues of β-*N*-acetylmuramic acid or α-*N*-acetylneuraminic acid on rAT virus are more involved in virus–cell interactions (Fig. 4b).

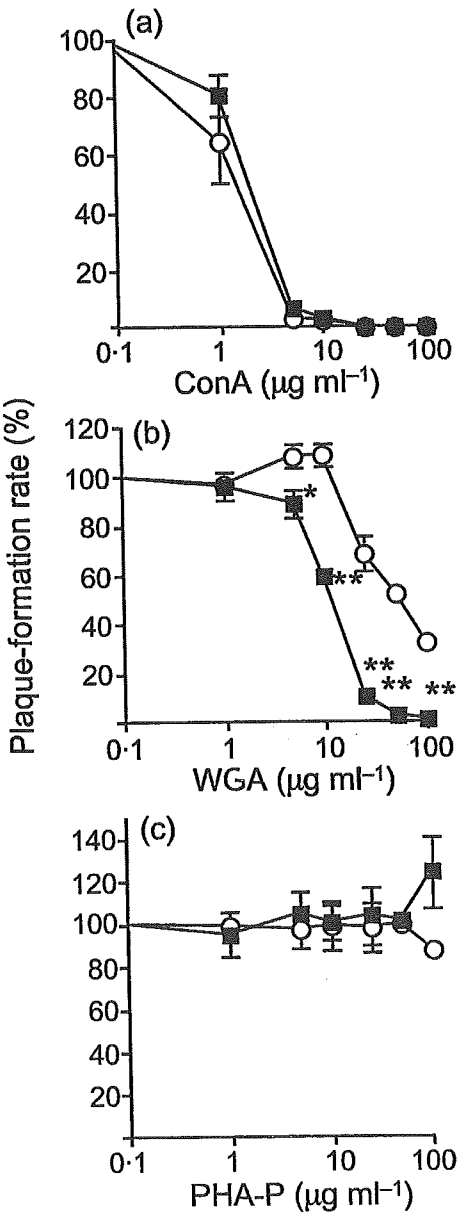

Fig. 4. Inhibition of viral internalization of rAT (■) and rAT-E138K (○) viruses into Vero cells with lectins: (a) concanavalin A; (b) wheatgerm agglutinin; and (c) phytohaemagglutinin P. Plaque-formation rates for each sample were examined. Each value represents the mean of three separate experiments. Error bars indicate SD. *, $P<0{\cdot}01$; **, $P<0{\cdot}001$.

Detection of endocytosis of recombinant JEV on Vero cells

Plaques of both rAT and rAT-E138K were effectively reduced by chlorpromazine on Vero cells (Fig. 5a). Plaque formation was inhibited more efficiently for rAT-E138K than for rAT at a concentration of 5 μg chlorpromazine ml^{-1} ($P<0{\cdot}05$). At a higher concentration of 20 μg ml^{-1}, about 20% of Vero cells dissociated due to cytotoxicity. This result indicates that clathrin-dependent endocytosis is involved in JEV infection. Plaque formation by rAT virus was reduced by about 20% by cytochalasin D at concentrations within the range 1–20 μg ml^{-1}, but the rAT-E138K strain was unaffected. Thus, macropinoendocytosis by Vero cells is more important for rAT than for rAT-E138K ($P<0{\cdot}05$; Fig. 5b). Furthermore, nystatin, an inhibitor of caveolae-mediated endocytosis, did not inhibit plaque formation of either the rAT or rAT-E138K strains (Fig. 5c). These results demonstrate that both rAT and rAT-E138K strains predominantly utilize penetration via clathrin-dependent endocytosis, rather than caveolae-mediated endocytosis, in Vero cells. The macropinoendocytosis function may also be involved in penetration of rAT virus, but not in that of rAT-E138K.

Recombinant virus release

Following JEV infection of Vero cells at an m.o.i. of 5 p.f.u. per cell, significantly higher titres of rAT virus were detected in supernatant compared with cell-associated virus at 24–48 h post-inoculation ($P<0{\cdot}05$; Fig. 6a). In contrast, higher titres of rAT-E138K virus were detected consistently in the intracellular fraction than in the supernatant. These significant differences in rAT-E138K virus titres between intra- and extracellular fractions were seen at all time points examined ($P<0{\cdot}05$; Fig. 6b). However, total amounts of replicated rAT virus and rAT-E138K virus were similar (Fig. 6c). These data demonstrate clearly that the point mutation significantly inhibits virus release from infected Vero cells, but does not affect virus replication.

On primary neural cells inoculated with JEV at an m.o.i. of 5 p.f.u. per cell, higher titres of rAT virus were found in supernatant than in cell-associated fractions from 18 h post-inoculation (Fig. 6d). Again, significant differences in rAT virus titres were identified between intra- and extracellular virus titres at 24–72 h post-inoculation ($P<0{\cdot}05$; Fig. 6d). In contrast, higher titres of rAT-E138K virus were also present in the intracellular fraction than in supernatant (Fig. 6e), and significant differences in virus titres were

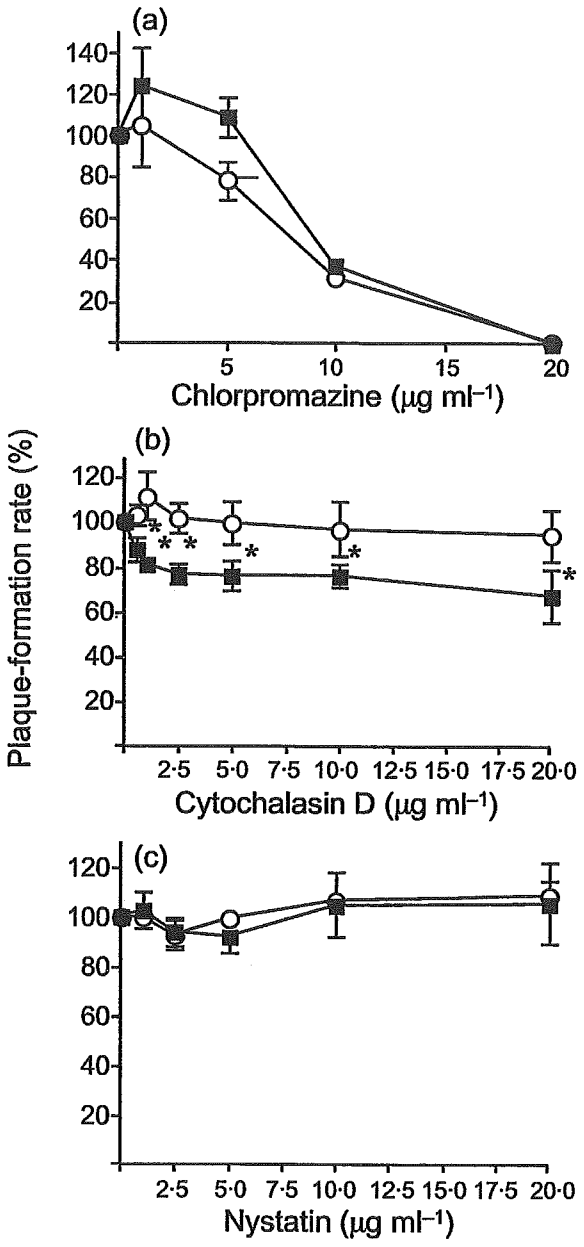

Fig. 5. Inhibition of recombinant JEV internalization on Vero cells. Endocytosis inhibition of rAT (■) and rAT-E138K (○) viruses was examined by using different concentrations of chlorpromazine (a), cytochalasin D (b) and nystatin (c). Each value represents the mean of three separate experiments. Error bars indicate SD. *, $P<0{\cdot}05$.

found between intra- and extracellular fractions at 12–72 h post-inoculation ($P<0{\cdot}05$; Fig. 6e). As with the results for Vero cells, no significant differences in total amounts of replicated virus were observed between rAT and rAT-E138K (Fig. 6f). These results indicate clearly that the point mutation significantly inhibits secretion of replicated virions from both infected Vero cells and primary neural cells.

DISCUSSION

Previous studies have indicated that irregular mutations often taken place at the 5′-end region of full-length JEV cDNA clones (Arroyo *et al.*, 2001; Sumiyoshi *et al.*, 1992; Yun *et al.*, 2003). Through insertion of short introns, the JEV infectious clone was constructed and was able to be propagated stably in *Escherichia coli* (Yamshchikov *et al.*, 2001). In our study, several unforeseen mutations also occurred when the full-length cDNA of AT31 virus was cloned into pBR and pUC vectors (T. Wakita, T. Date, Y. Li & K. Yasui, unpublished data). Focusing on this problem, the 5′-end fragment of JEV AT31 cDNA was cloned into the very low-copy-number pMW118 vector. By inserting another 3′ fragment of JEV, a full-length cDNA of JEV AT31, pMWJEAT, was successfully constructed and amplified. Sequence analysis of viral RNA isolated from the recombinant JEV rAT strain revealed no mutation compared with the template pMWJEAT.

By analogy with three-dimensional structure models of TBE virus (Rey *et al.*, 1995; Mandl *et al.*, 2001) and *Dengue virus* (Zhang *et al.*, 2003b), the E glycoprotein of JEV is predicted to contain an extended structure with seven β-sheets, two α-helices and three domains (Kolaskar & Kulkarni-Kale, 1999). The E glycoprotein is the viral haemagglutinin and induces protective immune responses and mediates receptor-specific viral attachment to cell surfaces. Previous reports have indicated that mutations in the JEV E protein affect viral neurovirulence or neuroinvasiveness *in vivo* (Yu *et al.*, 1981; Ni & Barrett, 1998) or viral binding and entry into cultured cells *in vitro* (Hasegawa *et al.*, 1992; Lee & Lobigs, 2002). The molecular basis of viral attenuation in flaviviruses has been analysed by using site-directed mutagenesis of infectious cDNA clones (Kinney *et al.*, 1997; Hurrelbrink *et al.*, 1999), production of chimeric viruses (Arroyo *et al.*, 2001) and deletions in the 3′ untranslated regions of genomes (Whitehead *et al.*, 2003). Residue 138 of the E protein has been considered to be located on the E0 β-strand in domain I and to be exposed on the surface of the E protein (Lee *et al.*, 2004). The data described in the present manuscript demonstrate that mutation of the E-138 residue in JEV from Glu to Lys inhibits viral spread from cell to cell, explaining the small-plaque morphology. Previous studies have indicated that mutations in domain III of the flavivirus E protein modulate virus binding and entry into host cells (Hung *et al.*, 2004; Liu *et al.*, 2004; Modis *et al.*, 2004). The dimer-to-trimer structural transition of the E protein induced by low-pH conditions is considered crucial for virus–cell binding and entry processes (Stiasny *et al.*, 1996; Chen *et al.*, 1997; Arroyo *et al.*, 2001) and this binding may be affected by mutations in the E protein. The E-138 mutation is not located in domain III, but enhances virus–cell attachment greatly under acidic conditions (Fig. 2).

Flaviviruses are considered to be internalized after binding to glycosaminoglycan (GAG) residues on cells, and other molecules are also involved in virus entry for some viruses

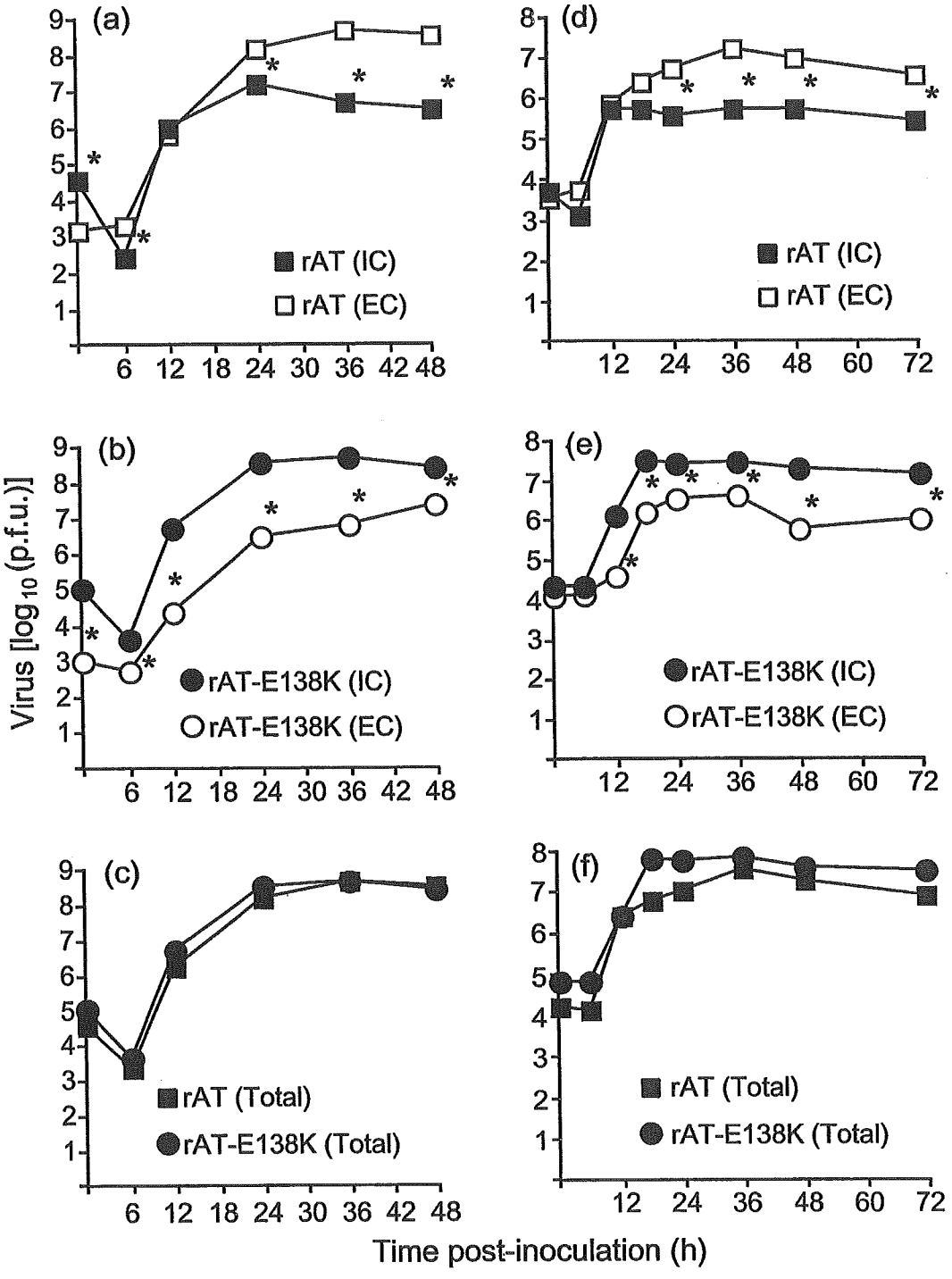

Fig. 6. Replication and secretion of rAT (■, □) and rAT-E138K (●, ○) viruses inoculated into Vero cells. JEV rAT and rAT-E138K strains were inoculated at an m.o.i. of 5 p.f.u. per cell into Vero cells (a–c) or primary neuron cells of BALB/c mice (d–f). Viruses released into the supernatant or retained in the cytoplasm were detected by plaque assay. IC, Intracellular; EC, extracellular; Total, total of intra- and extracellular virus. *, $P<0{\cdot}05$.

(Mandl *et al.*, 2001; Lee *et al.*, 2004; Liu *et al.*, 2004). The binding reaction can be inhibited *in vitro* by using heparin (Chen *et al.*, 1997; Hurrelbrink & McMinn, 2001; Lee & Lobigs, 2002). However, the molecular effects of heparin on virus-binding activity with JEV attenuation are not well understood. Previous studies have indicated that mutations of residues E-49, E-138, E-306 or E-389 on the JEV E protein reduce the efficiency of viral binding to heparan sulphate